FISFVIFR

Contents lists available at ScienceDirect

Journal of Hydrology: Regional Studies

journal homepage: www.elsevier.com/locate/ejrh



Extreme rainfall and temporal loading in Great Britain: Analysis of present and future trends using a convection-permitting climate model

Molly Asher ^{a,b}, Jonas Wied Pedersen ^{c,d}, Steven Böing ^b, Cathryn Birch ^b, Mark Trigg ^a, Elizabeth Kendon ^{e,f}

- ^a School of Civil Engineering, University of Leeds, Leeds, UK
- ^b Institute for Climate and Atmospheric Science, University of Leeds, Leeds, UK
- ^c Weather research, Danish Meteorological Institute, Sankt Kjelds Plads 11, 2100 Copenhagen O, Denmark
- d DTU Sustain, Technical University of Denmark, Bygningstorvet Building 115, 2800 Kgs. Lyngby, Denmark
- e School of Geographical Sciences, University of Bristol, United Kingdom
- f Met Office Hadley Centre, Exeter, UK

ARTICLE INFO

Keywords: Extreme rainfall Event temporal loading Climate change CPM UKCP18 Flood risk

ABSTRACT

Study Region: Great Britain

Study Focus: While climate change is intensifying rainfall extremes, its effect on temporal loading remains poorly understood. Temporal loading, the distribution of rainfall over storm duration, influences flood risk for storms of a given volume and is critical for urban infrastructure planning. This research presents the first direct investigation of event temporal loading within climate projections, utilising UKCP Local convection-permitting ensemble simulations. At rain gauge locations, we sample the most extreme storm each year at durations from 1.5 to 24 hours and apply two classification metrics to evaluate storm temporal structure.

New Hydrological Insights for the Region: Our analysis confirms that in today's climate, shorter-duration storms tend to be front-loaded, while longer storms exhibit more centred, symmetrical intensity profiles. Spatial patterns emerge with central and southern England exhibiting a higher proportion of highly asymmetric events. However, no consistent changes in temporal loading are projected under future climates, challenging previous inferences based on temperature–rainfall relationships. These discrepancies may stem from differences in storm-generating mechanisms between Great Britain and tropical regions studied previously. Our findings highlight limitations of current metrics, which inadequately distinguish aspects of storm structure contributing to temporal loading. We recommend developing refined metrics to independently quantify event asymmetry, peak intensity, and timing. Such advancements are crucial for improving design flood modelling alongside future climate scenarios.

1. Introduction

A defining feature of rainfall events is that intensity fluctuates over time as a storm evolves, driven by atmospheric dynamics, cloud processes, and moisture availability. Storms typically progress through phases of initiation, intensification, peak intensity, and dissipation, leading to distinct intensity profiles. These profiles are rarely uniform, with rainfall often concentrated in specific

https://doi.org/10.1016/j.ejrh.2025.102750

Received 2 May 2025; Received in revised form 28 July 2025; Accepted 27 August 2025

Available online 11 October 2025

2214-5818/Crown Copyright © 2025 Published by Elsevier B.V. This is an open access article under the CC BY license (http://creativecommons.org/licenses/by/4.0/).

^{*} Corresponding author at: School of Civil Engineering, University of Leeds, Leeds, UK. E-mail address: gy172ma@leeds.ac.uk (M. Asher).

periods rather than evenly distributed over the storm's duration. This variability is described in the literature using various terms, including the intensity profile (Dunkerley, 2021), storm profile (Kottegoda and Kassim, 1991), rainfall temporal pattern (Wang, 2020), or intra-event rainfall variability (Todisco, 2014). In this study, we use the term event temporal loading, and take this to refer to an event's temporal asymmetry, peakiness, and how concentrated rainfall is within small portions of the event.

Event temporal loading is a key driver of hydrological and geomorphological responses, and thus is of key importance in modelling flooding, as well as sediment transport (Liu et al., 2022; Dunkerley, 2021; Gao et al., 2024; Wang et al., 2023, 2016), pollution (Fu et al., 2021), and rainfall-induced landslides (Fan et al., 2020; Zhao et al., 2025). While the total rainfall volume within an event is the primary determinant of hydrological response, research across diverse settings has demonstrated that event temporal loading can substantially influence flood risk (Lambourne and Stephenson, 1987; Nguyen et al., 2002; Balbastre-Soldevila et al., 2019; Krvavica and Rubinić, 2020; Asher et al., 2025). For example, even when total rainfall remains constant, flood depth variations of up to 35% have been observed due to differences in temporal loading alone (Hettiarachchi et al., 2018). Additionally, later-peaking storms can worsen urban inundation (Li et al., 2021), and irregular rainfall distributions may disrupt drainage systems (Fadhel et al., 2018).

Research on observed rainfall events suggests there is considerable variation in event temporal loading (Pilgrim et al., 1969; Villalobos Herrera et al., 2023a; Ball et al., 2019), and that this variability appears to be related to storm characteristics such as event duration and magnitude. Despite this, pluvial flood modelling generally prioritises capturing the central tendency of storm patterns over their variability, and so generalised patterns are often applied, regardless of event duration or magnitude (Ball et al., 2019). For example, symmetrical, centrally peaked intensity profiles are common, such as the FEH design profiles in the UK and the Chicago design storm used in the US and other countries. While this approach is straightforward to implement, it fails to account for the actual diversity of event temporal loading patterns, which may lead to inappropriate design of urban rainfall infrastructure (Jun et al., 2021). The importance of addressing this limitation is likely to grow if the temporal loading of rainfall events shifts under climate change (Hathaway et al., 2024). The sensitivity of design hyetographs to such changes remains largely unknown (Watt and Marsalek, 2013), with progress hindered by uncertainties in the direction and magnitude of expected alterations to event temporal loading patterns (Ball et al., 2019; Peleg et al., 2020). Addressing these gaps is essential to ensure that flood modelling methodologies remain robust and relevant in a changing climate.

Climate change affects both the thermodynamics and dynamics of moist convection, with significant implications for rainfall patterns and flood risk. Thermodynamic changes are relatively well understood, with warming temperatures increasing atmospheric moisture-holding capacity at a rate of 6%–7% per degree Celsius of warming, as described by the Clausius–Clapeyron relationship (Trenberth et al., 2003). This leads to an expectation of intensified rainfall extremes, providing a thermodynamic baseline for projecting future changes (Westra et al., 2014; Barbero et al., 2017). However, some studies suggest that rainfall intensification may exceed Clausius–Clapeyron scaling at shorter timescales, a phenomenon known as super-Clausius–Clapeyron (super-CC) scaling (Lenderink and Van Meijgaard, 2009; Fowler et al., 2021). Super-CC scaling highlights the importance of understanding not only thermodynamic changes but also the dynamic processes that modulate storm behaviour and rainfall patterns. Dynamical changes, which involve shifts in storm structure, organisation, and behaviour, introduce significant uncertainty to projections of rainfall extremes (Peleg et al., 2020; Haerter et al., 2010). For instance, alterations in storm speed, convective cell development, and feedback mechanisms such as latent heat release (Lenderink and Van Meijgaard, 2009; Fowler et al., 2021) might be responsible for super-CC scaling and could potentially also influence the temporal distribution of rainfall within storms. These dynamical processes may interact with thermodynamic factors, further amplifying the intensity and variability of extreme rainfall events under climate change.

The influence of factors aside from temperature on temporal patterns means that there is limited evidence that the response of precipitation events to day-to-day climate variability will align with their response to warming (Fowler et al., 2021). Nevertheless, the limited research on how temporal rainfall patterns may change in future climates has often relied on historical relationships between temperature and rainfall as a proxy for future behaviour (Westra et al., 2014). Several studies have explored the possibility that rainfall intensification does not always occur uniformly throughout an event (Sharma et al., 2021). For example, Wasko and Sharma (2015) analysed historical rain gauge records and temperature measurements in Australia to investigate how temperature influences rainfall intensity across different fractions of a storm burst. Similarly, Fadhel et al. (2018) applied this method to a small number of rain gauges in West Yorkshire, UK. In both cases, higher temperatures were associated with less uniform temporal patterns, featuring more intense peaks. Supporting this, Long et al. (2021) observed that rainfall events in China become more temporally concentrated at higher temperatures, using their newly developed Temporal Concentration Index (TCI). The TCI quantifies the difference between an observed event's distribution and an assumed event with an even temporal distribution, with higher values indicating more concentrated rainfall. To the best of our knowledge, only two studies have explicitly addressed the link between rainfall event asymmetry and climate. Visser et al. (2023) investigated the relationship between temperature and precipitation loading in historical Australian rain gauge data, introducing a new metric, D50, which quantifies the proportion of an event's duration by which 50% of the total rainfall has occurred. Their findings suggest that rainfall extremes in tropical regions will become increasingly front-loaded in the future as temperatures rise. Ghanghas et al. (2024) expanded this analysis globally and applied a binary measure of event loading based on an assessment of the reversibility of the storm's temporal and spatial heterogeneity. Consistent with Visser et al. (2023), they showed that tropical regions are likely to experience more front-loaded rainfall events. However, they further identified a contrasting pattern in temperate, northern regions, where a shift towards increasing back-loaded events is expected.

The reliance on historical relationships to infer future changes in event temporal loading has been a pragmatic response to the limitations of coarse-resolution regional climate models (RCMs), which lack the spatial resolution needed to explicitly resolve deep

convective processes (Westra et al., 2014). These models rely on convection parameterisation schemes that, while somewhat capable of capturing average convective effects over large grid scales, struggle to simulate the timing, intensity, and spatial organisation of individual convective cells. In recent years, the emergence of convection-permitting regional climate models (CPMs), such as the UKCP Local (2.2 km) model, has begun to address these limitations (Dai et al., 2024). With resolutions fine enough to explicitly represent deep convection, CPMs eliminate the need for convection parameterisation. However, they still cannot resolve the smallest convective plumes and showers, leading to some unrealistic rainfall structures and biases, such as an overestimation of heavy rainfall intensity (Fosser et al., 2015). Despite these challenges, CPMs provide a much-improved representation of local-scale phenomena, including the initiation, maintenance, and dissipation of convective cells, as well as the occurrence of localised intense precipitation (Kendon et al., 2017; Prein et al., 2015; Fosser et al., 2020, 2015; Ban et al., 2014).

The UK Climate Projections convective-permitting ensemble simulations (UKCP Local), with 2.2 km spatial resolution, have been widely used to study various aspects of future rainfall events. For instance, Archer et al. (2024) used extreme events from UKCP Local to run simulations of rainfall-driven flooding for a case study near Bristol, showing the simulated flood impacts to be more severe than when based upon design rainfall with uplift factors applied. Chen et al. (2021) examined hourly extremes of convective summer storms, showing that future events are characterised by higher intensities, greater advection speeds, and larger spatial extents. Chan et al. (2023) developed spatially varying uplift factors for rainfall events with durations ranging from 1 to 24 h, and highlighted the value of these more precise regional values in properly quantifying changes to precipitation extremes. In earlier research, Chan et al. (2016) extracted rainfall extremes from a 1.5 km UK Met Office CPM over southern UK, focusing on extreme intensification with some analysis of event profiles. However, their method involved aligning event peaks centrally to construct composite mean profiles, artificially imposing symmetry and preventing assessment of event asymmetry.

Building on this prior work, the high-resolution, convection-permitting ensemble runs of UKCP Local offer a promising opportunity to directly study, for the first time, changes in the asymmetry of temporal patterns of sub-daily storms in climate projection data. To achieve this, we use 30-min rainfall data to sample the most extreme storm in each year for a range of durations (from 1.5 to 24 hours) and investigate key research questions:

- 1. How well does the model replicate the temporal loading of observed rainfall events at rain gauge locations?
- 2. Can spatial patterns be identified in the temporal loading of extreme events in both current and future climate scenarios?
- 3. Will the temporal loading of annual maximum events change in the future climate?
- 4. To what extent do existing metrics for quantifying temporal loading enable us to effectively answer these questions?

By examining these questions, we aim to advance understanding of how extreme rainfall events may evolve under climate change, supporting updates to flood modelling practices. Our findings seek to address the influence of shifting event temporal loading patterns on flood risk and encourage the adoption of methods that both reflect real-world variability and remain resilient to future climatic changes.

2. Data and methods

2.1. Data

The UKCP Local convection-permitting ensemble simulations, developed by the UK Met Office, provide high-resolution climate projections for the UK at a 2.2 km grid spacing for 12 ensemble runs. This study uses 30-min resolution outputs from these simulations, accessed through licence with the Met Office, for two time periods: a present-day baseline (2001–2019) and a future projection (2061–2079) under the high-emissions RCP8.5 scenario. The 2.2 km convection-permitting ensemble is nested within a regional climate model (HadREM3-GA705, referred to as the RCM) which spans Europe (Murphy et al., 2018), which is itself driven by the Hadley Centre global climate model (HadGEM3-GC3.05, referred to as the GCM), which runs at a 60 km resolution (Walters et al., 2019). The CPM is based on the Met Office's operational UK weather forecast model (UKV), employing a configuration similar to the Regional Atmosphere and Land Version 1 midlatitude configuration (HadREM3-RA11M) of the Met Office Unified Model (Kendon et al., 2019). Both the CPM and RCM are limited-area, atmosphere-only models, with prescribed daily sea surface temperatures and sea ice cover from the driving global simulation (Kendon et al., 2023). While the CPM and RCM share similar model physics, the CPM explicitly represents convection and the convection parameterisation scheme is turned off. Each CPM ensemble member is driven by unique boundary conditions from its corresponding RCM member (Kendon et al., 2023). However, unlike the RCM and GCM ensembles, which perturb parameters in their model physics to introduce variability, the CPM uses an identical model configuration across all members. The CPM ensemble thus consists of 12 random realisations of the same climate model and does not fully sample the range of uncertainties in convective-scale processes (Fosser et al., 2020).

In October 2024, the Met Office issued guidance highlighting that the 2.2 km UKCP Local simulations contain a small number of extreme rainfall values with physically unrealistic shapes and intensities (UK Met Office, 2024). The cause of these anomalies is not fully understood, and no robust correction method has been established. Regridding to 5 km reduces the impact of the unphysical events due to spatial smoothing. Following Met Office recommendations, we reproduced all analyses using the 5 km regridded data to assess sensitivity. Differences in temporal loading plots were minor, showing a slight reduction in asymmetry consistent with expectations from spatial smoothing. These findings suggest that the 2.2 km data remain broadly reliable for our analysis. As the finer resolution is critical for capturing temporal loading in greater detail, we present results based on the 2.2 km simulations. Sensitivity test results are provided in the Supplementary Material.

The hourly CPM projections have been previously validated against CEH-GEAR hourly gridded observations (Lewis et al., 2018) across Great Britain. The seasonal and annual maximum hourly precipitation values show good agreement with the observations, as do the frequency of events exceeding high thresholds (Kendon et al., 2023). Despite some remaining deficiencies, including the tendency of heavy rainfall to be overly intense in summer, this agreement supports the credibility of the CPM in accurately representing convection and short-duration precipitation extremes. We additionally validate the 30 min simulated data against rainfall rates from the NIMROD product which processes radar rainfall estimates from the UK Met Office weather radar network (Met Office, 2003; Harrison et al., 2000, 2012). Radar rainfall rates are aggregated to mean values over 30 min and hourly periods. A cumulative probability distribution of precipitation intensities is plotted, featuring the UKCP Local simulated data at both 30 min and hourly resolution, the NIMROD rainfall rates at both 30 min and hourly resolution, and CEH-GEAR at hourly resolution.

We constrain our model analysis to the locations of 1291 rain gauges across Great Britain where temporal patterns were previously examined for the present climate by Villalobos Herrera et al. (2023a). Given that the event set for these locations alone spans over two million events for each of the present and future climate time slices, assessing the full model grid would have been computationally infeasible. Additionally, this approach facilitates comparison with Villalobos Herrera et al. (2023a)'s findings on rainfall characteristics at the same locations. To map each rain gauge to its corresponding grid cell, a k-d tree algorithm was used to perform a nearest-neighbour search among the grid cell centre points.

2.2. Methods

2.2.1. Rainstorm definition and sampling

The way extreme precipitation events are defined can significantly influence assessment of how they respond to warming (Pendergrass, 2018; Schär et al., 2016). In this research, we opt to study the annual maximum rainfall accumulations at each rain gauge location associated with several durations of relevance to flood modelling ($N = \frac{1}{2}$ -, 1-, 2-, 3-, 6-, 12-, and 24-h). For each 2.2 km grid box, the heaviest rainfall over an *N*-hour period is located using a rolling window analysis, where each *N*-hour segment of the time series is evaluated sequentially. The 30-min window with the highest cumulative rainfall is identified as the core of the storm.

From the core, we perform a series of outward searches to identify the complete, independent rainfall event which the core is nestled within. We apply the search algorithm from Villalobos Herrera et al. (2023b), adapted for 30-min model data rather than 5-min rain gauge data. The first stage examines 30-min intervals before and after the core, adding those with rainfall >0.2 mm until encountering an interval with less. The second stage examines hourly intervals before and after the updated core, and adds those with combined rainfall >0.4 mm, until encountering an hourly interval with less. The final stage ensures the event is independent from nearby rainfall events. Ensuring event independence is crucial in hydrological modelling but can be challenging to implement (Ball et al., 2019; García-Bartual and Andrés-Doménech, 2017). A common approach defines independence through a rainfall-free interval before and after an event, known as the minimum inter-event time (MIT) (Restrepo-Posada and Eagleson, 1982; Molina-Sanchis et al., 2016). In the final search, rainfall values >1 mm within the MIT of the current event's start or end are included, with the search continuing iteratively until no further qualifying values are found. The MIT values used here are spatially variable and range from 3 to 19 h. They were calculated by Villalobos Herrera et al. (2023b) using a Poisson-based algorithm that identifies the minimum duration at which rainstorm arrival times become exponentially distributed (Restrepo-Posada and Eagleson, 1982). MIT values in other studies range from 3 min to 24 h and vary depending on the region's climatology or the intended use of the data (Rahman et al., 2002; Dunkerley, 2008; Molina-Sanchis et al., 2016).

The events for each ensemble member are extracted separately and then pooled together, giving annual maxima-producing events from 228 simulated years in both the present and future. The analysis is conducted on the full set of events comprising those producing annual maxima at any of the seven durations, and additionally storms are categorised based on their total duration into bins of ≤ 7 h ('short-duration storms'), 7–16 h ('mid-duration storms') and >16 h ('long-duration storms'). It is possible, and indeed probable, that in some cases the same rainfall event produces the annual maxima for multiple durations. When collating the set of annual maxima producing events for all durations, any duplicated copies of events are removed from the analysis. Any events less than 1.5 h (including less than three data points) are unsuitable for temporal analysis and are also discarded.

2.2.2. Event summary statistics

Rainstorm properties, including volume, intensity, and duration, are examined using density distributions to characterise their variability. The mean seasonality of annual maximum events are determined using circular statistics (Mardia, 1975; Hall and Blöschl, 2018; Bayliss and Jones, 1993). In this approach, the mean day-of-year of events, D_i , at a location is calculated by firstly converting the day-of-year of each event in Julian days, D_i , into an angular value, θ_i , representing its location on a unit circle, using the formula described by (Reed and Robson, 1999):

$$\theta_i = D_i \times \frac{2\pi}{m} \tag{1}$$

where m is the number of days in a year. The mean day-of-year as an angular value, $\overline{\theta}$, is then calculated as:

$$\theta_{i} = \begin{cases} \arctan\left(\frac{\overline{y}}{x}\right), & if \overline{x} \ge 0, \overline{y} \ge 0, \\ \arctan\left(\frac{\overline{y}}{x}\right) + \pi, & if \overline{x} < 0, \\ \arctan\left(\frac{\overline{y}}{x}\right) + 2\pi, & if \overline{x} \ge 0, \overline{y} < 0. \end{cases}$$
(2)

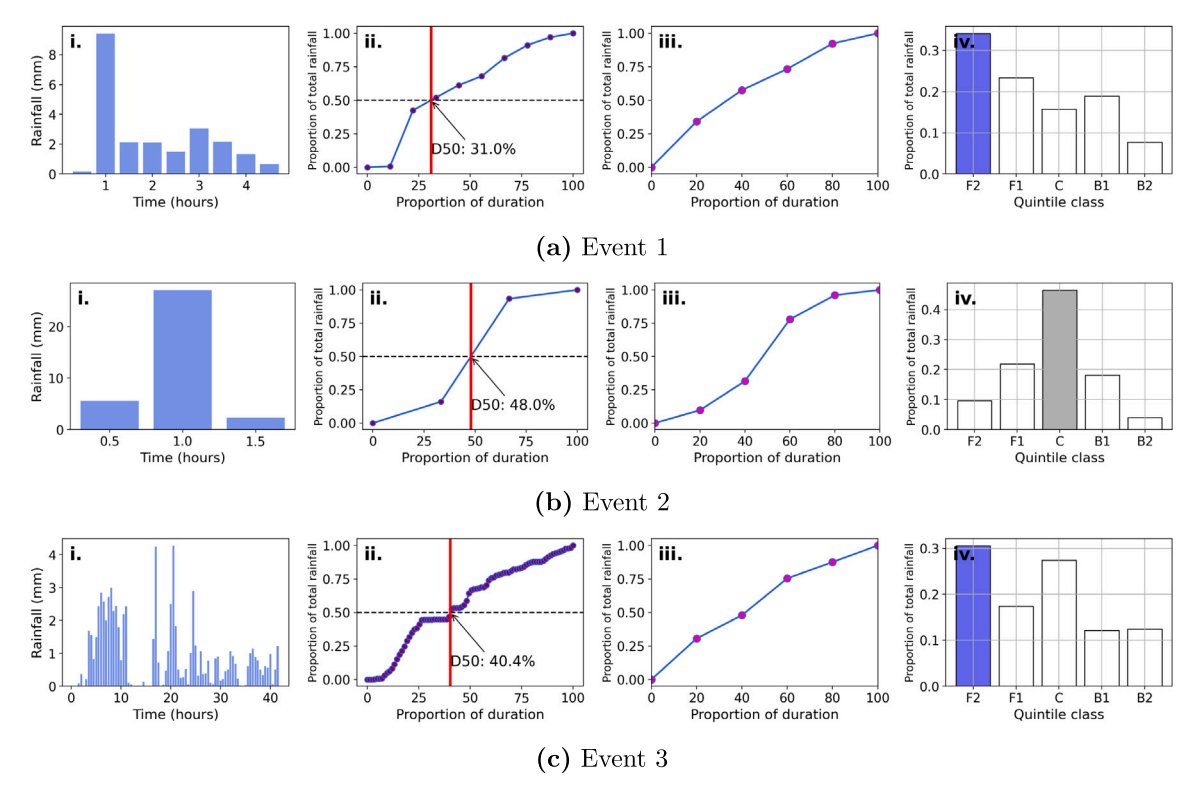


Fig. 1. Illustration of the event classification process based on the D_{50} metric and quintile classification, for three events. The figure shows (a) the raw rainfall data, (b) a dimensionless cumulative rainfall curve (with the calculated D_{50} metric indicated by the red line), (c) an interpolated cumulative rainfall curve with five resampled data points, and (d) the derived quintile classifications that categorise the distribution of rainfall within each event. (For interpretation of the references to colour in this figure legend, the reader is referred to the web version of this article.)

where \bar{x} and \bar{y} are two auxiliary variables representing the mean of the x-coordinates and mean of the y-coordinates, respectively, calculated as:

$$\bar{x} = \frac{1}{n} \sum_{i=1}^{n} \cos(\theta_i) \tag{3}$$

$$\bar{y} = \frac{1}{n} \sum_{i=1}^{n} \sin(\theta_i) \tag{4}$$

Finally, the mean circular direction is converted to a Julian day by multiplying by $\frac{365.25}{2\pi}$. Additionally, *R*, the concentration of seasonal distribution (Mardia, 1975; Blenkinsop et al., 2016) is calculated as:

$$R = \sqrt{\bar{x}^2 + \bar{y}^2}, \quad 0 \le R \le 1 \tag{5}$$

where an R value close to 1 is strongly seasonal, and D_i is therefore meaningful, and where R is closer to 0 then there is no strong seasonality to event occurrence, and therefore D_i has less importance (Villarini, 2016).

For analyses based on the mean day-of-year of events at locations (Figs. 5 and 10), we encounter the issue that the mean value at some locations is in January (see Supplementary Fig. A.2). In analyses that rely on a linear, rather than circular, representation of time, these dates appear numerically distant from those occurring at the end of the year, despite being temporally very close. This can create challenges in detecting linear trends and modelling relationships with other variables. To address this, we add 365 to all days-of-year in January and define a pseudo-year beginning at the start of February. The absence of annual maxima during the spring months creates a natural 'gap' in the circular representation of the calendar year, further supporting the logic of this approach.

2.2.3. Event loading analysis

Two methods are used to classify the event temporal distribution. Fig. 1 provides an illustration of how these methods are computed for three hypothetical rainfall events. To compare rainfall events of different durations, dimensionless mass curves are

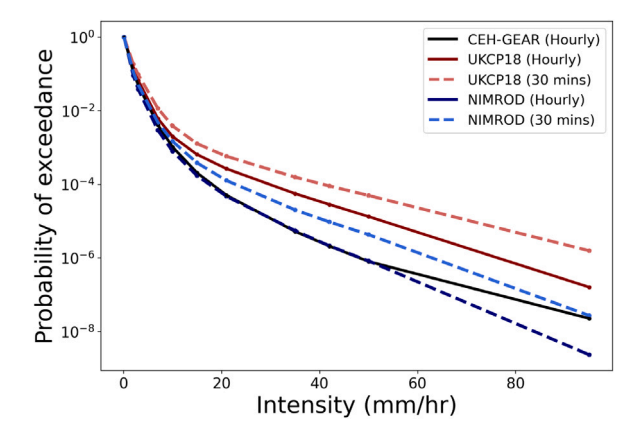


Fig. 2. Cumulative probability distribution of hourly precipitation intensity, for wet values (>0.1 mm/h) for the whole year across 2.2 km grid cells over Great Britain. NIMROD data is aggregated from 5 min values to 30-min and one hour. Before aggregation values >300 mm/h are removed. Figure shows the probability of exceeding the relevant intensity levels. For UKCP Local the data covers the present time period used throughout this study of 2001–2019, the NIMROD radar 30 min and hourly data is for 2006 to 2019, and CEH-GEAR for 1990–2016.

created. Each event's raw rainfall data (Fig. 1a) is transformed into a dimensionless format, representing the percentage of storm duration against the percentage of cumulative rainfall (Fig. 1b, purple dots) (Huff, 1967; Bonta and Shahalam, 2003).

The first method applies the D_{50} metric from Visser et al. (2023), which identifies the point in time at which 50% of the total rainfall has occurred. This is calculated by linearly interpolating between points on the dimensionless cumulative rainfall curve (Fig. 1b, blue lines). The D_{50} value is determined (red vertical line in Fig. 1b) where the interpolated line intersects the 50% cumulative rainfall threshold (Fig. 1b, black dashed line). The second method, based on Villalobos Herrera et al. (2023a), identifies the fifth of the event that contains the most rainfall. After linearly interpolating the cumulative rainfall curve, five evenly spaced points are resampled (Fig. 1c, pink dots). This allows us to calculate the proportion of the total rainfall falling within each 20% segment of the event's duration (Fig. 1c). The segment with the highest rainfall is labelled based on the following classification: F2 (first 20%), F1 (second 20%), C (middle 20%), B1 (fourth 20%), and B2 (final 20%) (Fig. 1d). Here, F, C, and B denote 'front', 'centre' and 'back'.

Note that the two methods can yield substantially different outcomes, as seen in Event 1. This is because the D_{50} metric reflects the centre of mass of the precipitation, and depends on how precipitation is distributed throughout the duration of the event. In contrast, the quintile classification focuses only on the segment with the highest rainfall, and does not account for the overall precipitation centre of mass. In this study, we apply both metrics to explore the extent to which the choice of metric may lead to differences in outcome.

3. Results and discussion

3.1. Climate model validation

Fig. 2 presents a validation of the probability of exceeding rainfall intensities in the UKCP Local (2.2 km) 30-min data against multiple reference datasets. These include UKCP Local (2.2 km) hourly data, CEH-GEAR hourly gridded observations (regridded from 1 km to 2.2 km), and NIMROD radar-derived rainfall rates at both 30-min and hourly resolutions (also regridded from 1 km to 2.2 km). Consistent with the findings of Kendon et al. (2023), UKCP Local exhibits a wet bias in simulated hourly values compared to CEH-GEAR observations. In addition, we show here that NIMROD hourly rainfall rates align closely with CEH-GEAR except at intensities >50 mm/hr. As expected, the 30-min NIMROD data shows higher intensities than its hourly counterpart due to the smoothing effect of temporal averaging, which reduces peak values over longer periods. Notably, the difference between the 30-min and hourly data is comparable for both NIMROD and UKCP Local, suggesting that the influence of temporal averaging is similarly represented in the UKCP Local data. Additionally, the gap between the hourly observation datasets (CEH-GEAR and NIMROD) and UKCP Local hourly data is similar to the gap observed between the NIMROD and UKCP Local 30-min data, indicating that the wet bias in UKCP Local is consistent across temporal resolutions. These consistencies provide confidence in the reliability of the UKCP Local 30-min data for further analysis.

3.2. Rainstorm properties

UKCP Local future projections indicate a general tendency for annual maxima to shift towards higher rainfall intensities and volumes (Fig. 3). This aligns with simulations of sub-daily extremes in other convection-permitting models, as discussed in Grabowski and Prein (2019).

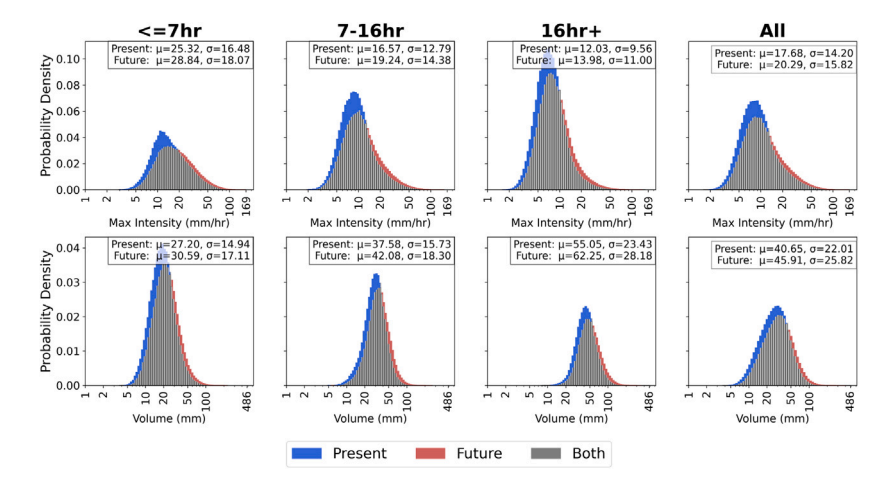


Fig. 3. Density distributions for event (a) maximum intensity and (b) volume. Results displayed for all events and for three event duration categories.

3.3. Rainstorm seasonality characteristics

Fig. 4 shows how extreme events of different durations are distributed seasonally in both the present and future climates. In the present climate, short-duration extremes are strongly concentrated in summer, with a clear peak between June and August. This is consistent with current data from rain gauges, which show that short-duration extremes in the UK most often occur during the summer (Blenkinsop and Fowler, 2014; Darwish et al., 2018). Mid-duration events, on the other hand, are more evenly spread across both summer and autumn, while long-duration events happen throughout the year, with autumn and winter including the most annual extremes. In the future climate, the patterns shift substantially. For short- and mid-duration events, the seasonal concentration decreases, with fewer events occurring in summer and more shifting to autumn. In contrast, the seasonal concentration of long-duration events increases, with autumn and winter events becoming more frequent.

The mean day-of-year for annual maxima at each sampling location is shown in Fig. 5, revealing spatial variation in seasonality. For short-durations, the range of values across different locations is relatively narrow, spanning from June to September. For longer events, the mean day-of-year varies more widely, ranging from July to December for mid-duration, and from October to January for long-duration events. For all durations, the latest annual maxima are often observed along the southern and western coasts, as well as in Scotland for the longest-duration events. These patterns align with some findings from previous research: Dales and Reed (1989) observed that locations in the south west of England had the latest mean day of occurrence for daily annual maxima, and Jones et al. (2013) found that events on the east coast tended to occur in summer, whereas those further inland were more common in autumn. Similarly, Ledingham et al. (2019) found that daily annual maxima occurred later in the year in Scotland and Wales, and earlier in England, which broadly corresponds with our results, particularly for the southern and western coasts and Scotland for long-duration events. However, there are some differences, particularly along the southern coast of England and the Pennines.

Understanding these seasonal shifts in extreme rainfall timing is important for both flood risk and water resource management. Regions where annual maxima occur later in the year may experience higher flood risks during winter, when soil saturation and river levels are already elevated, exacerbating runoff generation. Additionally, in urban areas, extreme rainfall events that occur later in the year may coincide with periods of reduced drainage efficiency, as fallen leaves and other debris can block drainage systems, further exacerbating flood risks. Conversely, summer-dominated maxima in some regions may indicate an increased risk of intense convective storms, which can overwhelm urban drainage systems that are unable to cope with the growing peakiness of events. These findings highlight the need to incorporate seasonal shifts in rainfall extremes into urban flood risk assessments and infrastructure design, ensuring that drainage capacity, emergency response planning, and adaptation strategies remain effective under changing climatic conditions.

The spatial variation in seasonal concentration, *R*, which is key to interpreting the mean day-of-year, is plotted in Fig. A.1 in the supplementary material. For short-durations, seasonal concentration is high at all locations, although particularly pronounced in the north. This suggests that across locations the mean day-of-year values are representative of the mid-point of a seasonal peak. For mid- and long-durations, seasonal concentration is consistently lower across Great Britain than it is for short-durations. Consequently, the mean day-of-year values in Fig. 5 for these durations represent the mid-points of fairly wide distributions rather than indicating distinct seasonal peaks. For the longer durations especially, seasonal concentration values are higher around the southern and western coasts, coinciding with the areas with the latest mean day-of-year values.

There are clear spatial patterns in changes in the future climate in the mean day-of-year (Fig. 5) and the seasonal concentration, R (Fig. A.1), at locations across Great Britain. The shift of annual maxima to later in the year is the least substantial for short-and mid-durations. In northern England and Scotland many locations exhibit no noticeable shift for these durations, and some even

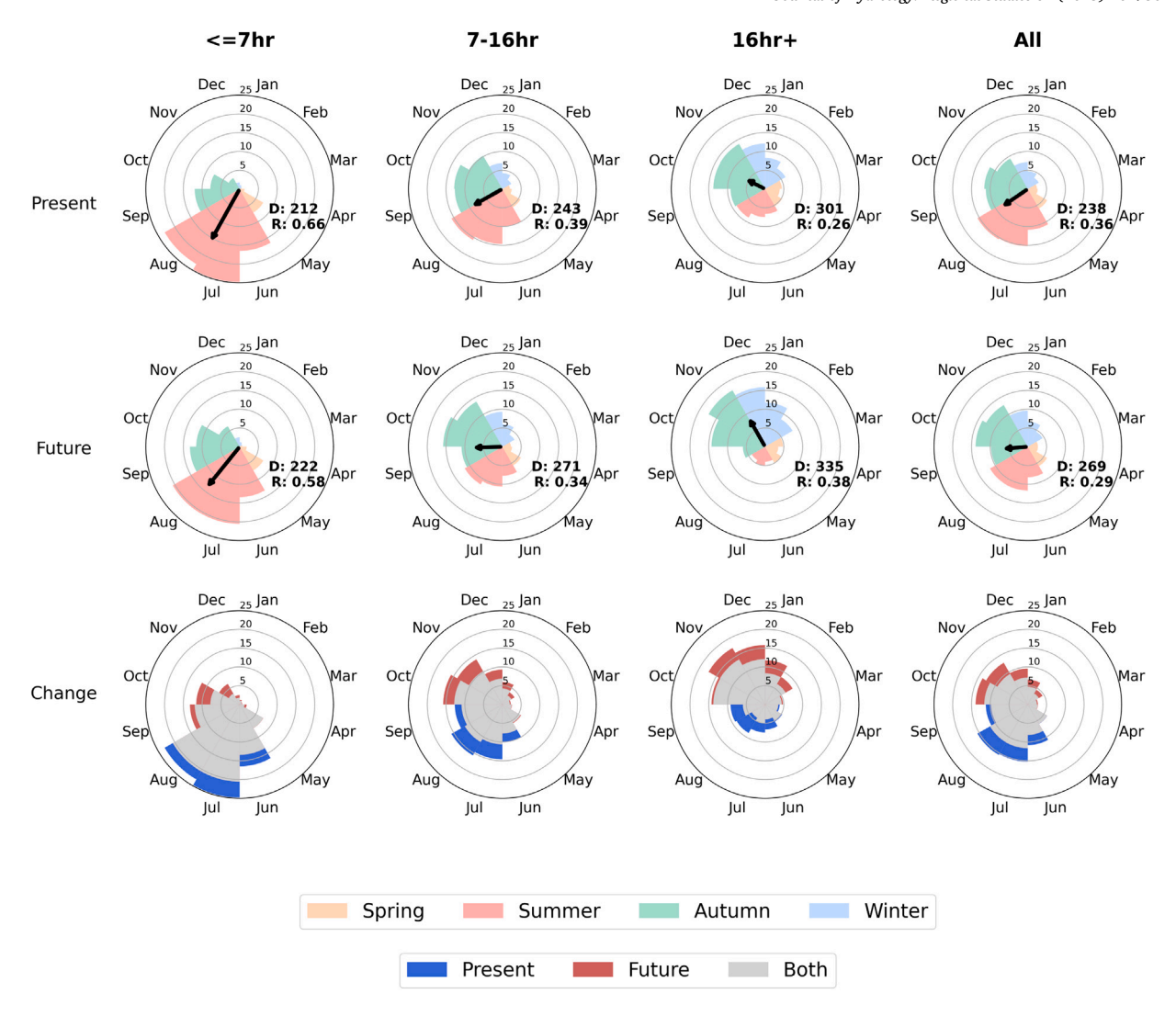


Fig. 4. Temporal distribution of annual maxima rainstorms across all locations. Results are displayed for present (2000–2019) and future climates (2060–2079) and the difference between the two, and for all events and for three event duration categories. Arrow indicates the direction and strength of the seasonal concentration (R). The mean event day-of-year value and an R value are printed in text.

show a tendency for events to occur earlier in the year. For long-durations, locations in central and eastern England see the largest shift in the timing of events. In terms of R, for short-durations, locations in northern England and Scotland are again less likely to experience a change. For mid- and long-duration events, R increases in Wales, western Scotland and the south of England, and decreases strongly in other parts of central England. For both R and the mean day-of-year, the regions that deviate from the trend of events shifting later in the year and becoming less seasonally concentrated, appear to, at least partially, correspond with areas of higher elevation, such as the North Pennines, the Welsh mountains, and northern Scotland.

The decreasing predominance of summer events in the annual maxima collection aligns with results from Chan et al. (2020), who used the high-resolution (2.2 km) UK Met Office Unified Model CPM over a pan-European domain to investigate future rainfall extremes. Mirroring the patterns seen in our study, Chan et al. (2020) observed a flattening of the seasonal cycle in a warmer climate, marked by a shift in the mean day of occurrence towards autumn. A declining proportion of extreme events in summer has also been observed in the historical rain gauge record over the past 50 years, suggesting this process is already underway (Prosdocimi et al., 2014). This can be attributed to several factors. First, evidence suggests that winter frontal events are getting heavier and will continue to do so in the future (Cotterill et al., 2021; Blenkinsop and Fowler, 2014; Sexton et al., 2024; Berthou et al., 2022; Kendon et al., 2014; Chan et al., 2020). This trend has been linked by Prosdocimi et al. (2014) to a persistent strong phase of the North Atlantic Oscillation (NAO). A high NAO index is associated with more intense winter frontal rainfall, driven by strong westerly winds, and less intense summer rainfall, as milder air masses suppress convection (McKenna and Maycock, 2022). Moreover, climate models generally predict that under a high-emissions scenario the winter NAO index will increase by the end of the century (Lee et al., 2021;

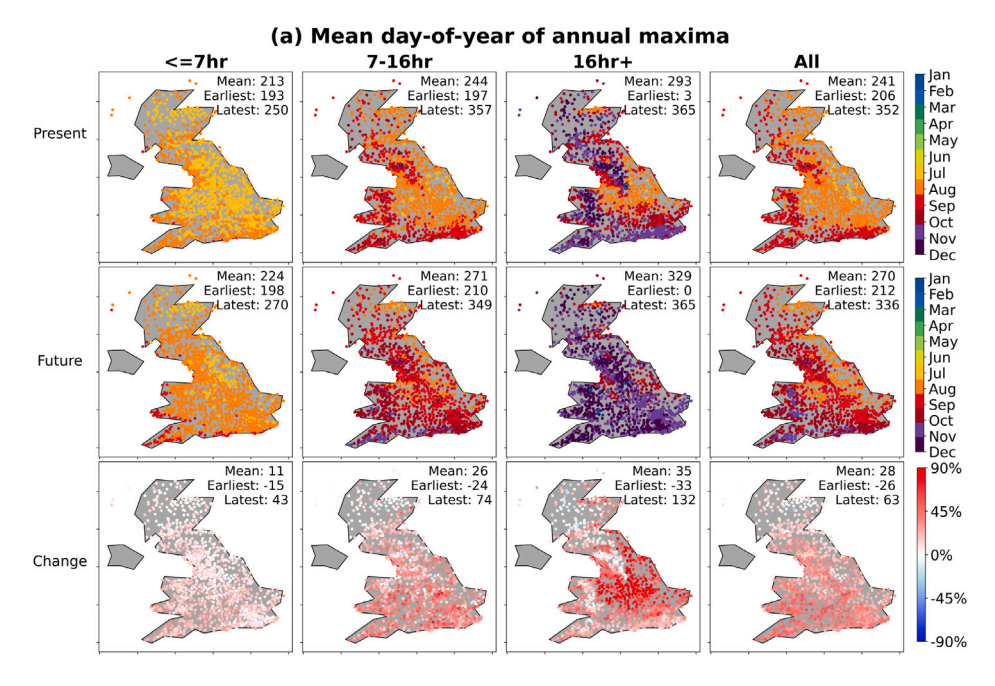


Fig. 5. The mean day-of-year of events extracted from UKCP Local climate simulations at grid box locations containing rain gauges. Results are displayed for present (2000–2019) and future climates (2060–2079), for all events and for three event duration categories.

Gillett and Fyfe, 2013; Stephenson et al., 2006). Combined, these factors increase the likelihood of frontal events dominating the annual maxima. It is possible that the coincidence of locations undergoing no change in event seasonality and elevated topography, is because frontal events were already dominant in these areas. Another possible explanation for the shift towards annual maxima occurring later in the year is the extension of the convective season into autumn. Studies show that summer weather regimes are persisting later into the year and beginning earlier (Vrac et al., 2014). Similarly, UKCP Local temperature projections reveal an extension of the summer dry season, characterised by more frequent drier, summer-like conditions, into autumn (Cotterill et al., 2023). These inferences about the kind of events we are sampling is also useful for interpreting the event temporal loading results, as discussed more in Section 4.

3.4. Comparison of temporal loading metrics

The conclusions drawn about the predominance of different event temporal loading structures are sensitive to the choice of metric. The differing sensitivities of these metrics are evident in the proportion of events assigned to each category (Fig. 6a, b). For 'All' events, the quintile classification produces a flat-topped distribution, with middle categories dominating and proportions gently declining towards the extremes, though highly asymmetric events (F2 and B2) remain relatively common. In contrast, the D_{50} distribution is more centred with lighter tails. Across all event durations, D_{50} consistently classifies a higher proportion of events as centred and fewer as highly asymmetrical compared to the quintile method, with this effect becoming particularly pronounced for longer-duration events, where extreme asymmetry is notably rare under the D_{50} metric.

Further, Fig. 6c illustrates the spread of D_{50} values within each quintile category, highlighting the disparity between the two methods. If the methods were measuring the same thing, one would expect D_{50} values to align better with the quintile ranges (0–20 for F2, 20–40 for F1, and so forth). However, while D_{50} values generally centre around their expected ranges, considerable overlap occurs between adjacent categories. The methods show the greatest consistency in the C category and the greatest divergence in the most asymmetric categories, F2 and B2. Notably, some 'outlier' events in the boxplot are classified very differently depending on the method used, emphasising the importance of understanding how these metrics influence event characterisation.

The differences between these metrics arise from their contrasting sensitivities to storm structure. The quintile classification method classifies events based on the timing of peak rainfall alone, making it highly sensitive to isolated bursts of intense rainfall, even if the rest of the event is more balanced. In contrast, D_{50} accounts for the full distribution of rainfall over the event duration, meaning it is less influenced by short-lived peaks and more reflective of overall rainfall balance. This distinction explains why highly asymmetric storms (F2/B2) appear more common under the quintile method, whereas D_{50} produces a more centred distribution with fewer extreme cases. These differences are particularly pronounced for longer-duration events, where multiple bursts of rainfall tend to shift the centre of mass towards the middle, reducing the apparent prevalence of strongly asymmetric events under D_{50} .

These findings highlight the importance of recognising that different metrics of event temporal loading do not measure the same aspects of rainfall distribution equally. Event temporal loading encompasses multiple characteristics, including asymmetry,

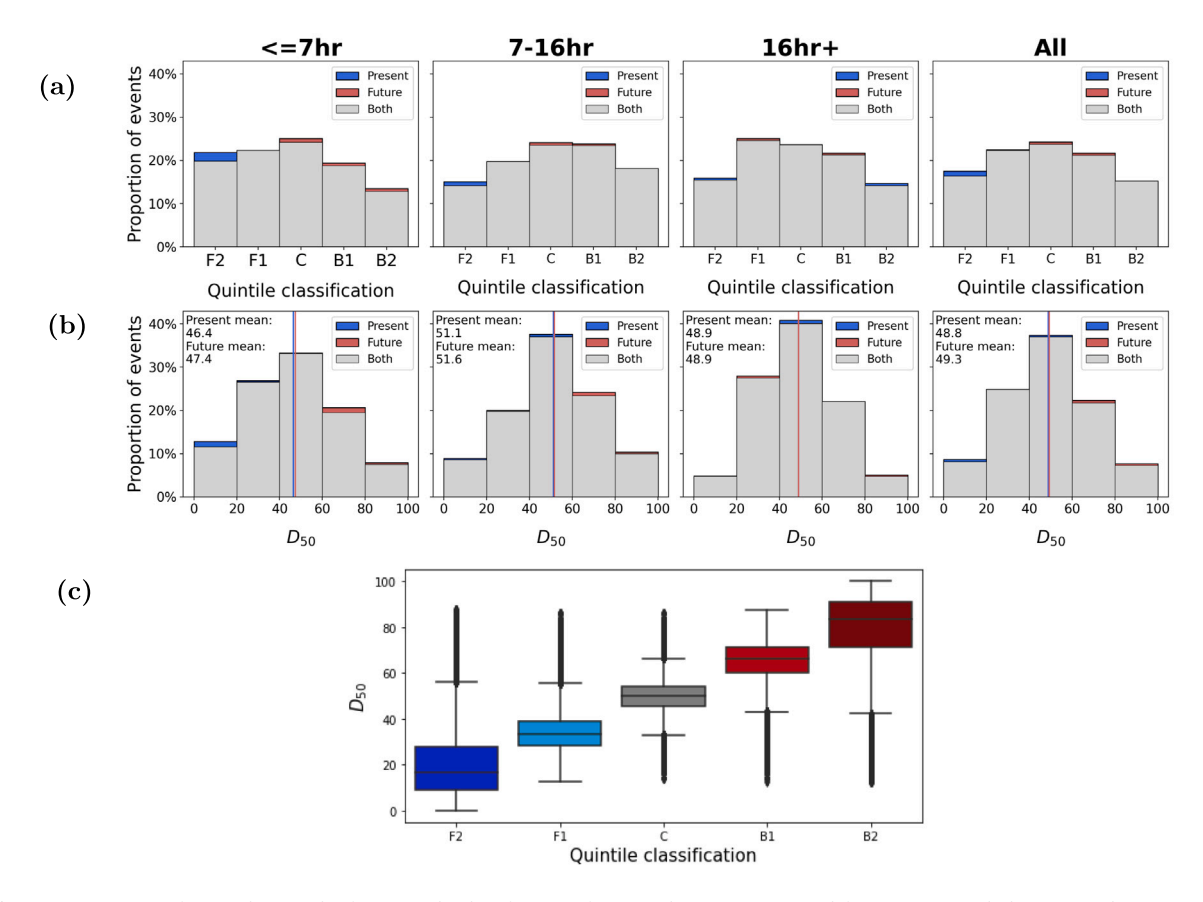


Fig. 6. Comparison of D_{50} values to the five quintile classifications for annual maxima extracted from UKCP Local climate simulations at grid box locations containing rain gauges, for a present (2000–2019) and future (2060–2079) climate. Proportion of annual maxima within (a) each of the five quintile classifications and (b) each of D_{50} categories binned to also include five categories. Vertical lines show the mean D_{50} for each of present and future climate. (c) Distribution of D_{50} values within the five quintile classifications for the present-day.

peakiness, and the concentration of rainfall within an event, but the relevance of these elements depends on the application. For example, in flood modelling, the timing and magnitude of peak intensity may be most critical, as they directly influence runoff generation. In contrast, soil erosion studies may be more sensitive to the concentration of intense rainfall over short durations. The choice of metric therefore shapes how event characteristics are represented and interpreted across disciplines. A single measure of event temporal loading is unlikely to be universally applicable, making it essential to either use multiple metrics or carefully select the one most suited to the specific process being studied to ensure robust event characterisation.

3.5. Analysis of event temporal loading

3.5.1. Overall findings

We find that in both the present and future the temporal loading of storms is influenced by event duration, agreeing with the results of both Villalobos Herrera et al. (2023a) and Visser et al. (2023). Fig. 6a shows the proportion of events in each quintile category for the different duration categories. We observe that short-duration events (≤7 h) tend to be front-loaded, with nearly half of these events falling into the front-loaded quintile categories (F1 and F2) and only around a third classified as back-loaded (B1 and B2). These findings align with Villalobos Herrera et al. (2023a), who reported that roughly half of short-duration storms sampled from gauges in Great Britain were front-loaded, being classified as either F2 or F1. This is supported by literature suggesting that short-duration storms are typically convective and peak in rainfall intensity early (Müller et al., 2017; Eagleson, 1970; Visser et al., 2023). For mid-duration events (7–16 h), the pattern flips, with front-loaded events becoming less common and back-loaded events more frequent. In the longest duration events (16+ h), there is a smaller proportion of highly asymmetrical events (F2 and B2), and although events are fairly evenly distributed across the middle three quintile categories, front-loading occurs slightly more often than back-loading. Again, this broadly aligns with Villalobos Herrera et al. (2023a) who found in rain gauge data that long-duration events were more likely to exhibit centred profiles and show less temporal variability.

The distribution of events across the five D_{50} categories differs noticeably from that of the quintile categories, as discussed in Section 3.4. Nevertheless, the overall conclusions regarding the differences in loading across durations remain largely consistent

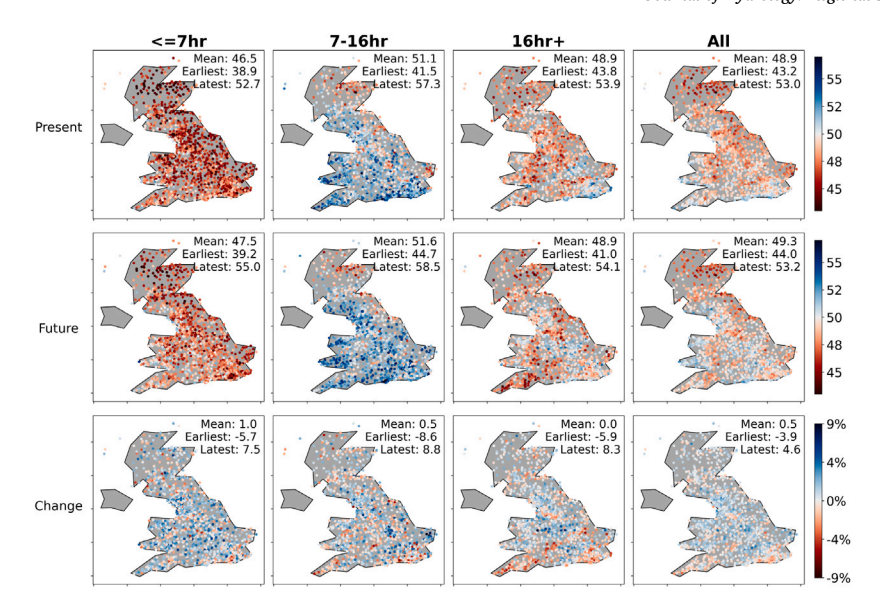


Fig. 7. The mean D_{50} value of annual maxima extracted from UKCP Local climate simulations at grid box locations containing rain gauges. Results are displayed for present (2000–2019) and future climates (2060–2079), for all events and for three event duration categories.

between the two methods. Fig. 6b illustrates that short-duration events exhibit the lowest mean D_{50} values and are most strongly front-loaded. Long-duration events also have a mean D_{50} below 50 and display higher proportions in the front-loaded compared to back-loaded categories. In contrast, mid-duration events are more inclined towards back-loading, with a mean D_{50} exceeding 50. Very little change is observed in future temporal loading with either the D_{50} metric or quintile classification (Fig. 6a).

3.5.2. Spatial patterns

Fig. 7 illustrates the average D_{50} value for events across different duration categories at each sampling location. The general trends align with Fig. 6a, where shorter durations exhibit the lowest mean D_{50} values, longer durations also show values below 50, and mid-duration events have slightly higher values just above 50. However, the plot also reveals that these overall trends hide specific spatial variations in event temporal loading. Across short-mid durations, northern and eastern areas generally exhibit lower mean D_{50} values. For longer durations, spatial patterns are less distinct, though higher values tend to cluster in the south east. These spatial differences are important because they indicate that event temporal loading is not uniform across the country, meaning that flood risk assessments or infrastructure design based on a single representative hyetograph may not fully capture local variations in storm structure. Recognising these patterns can help refine regional design guidelines and improve the accuracy of hydrological impact assessments under future climate scenarios.

The spatial distribution of the quintile classifications reveals slightly different patterns (Figs. 8, and A.3, A.4, A.5, A.6 in the supplementary material) experienced at each sampling location. At short durations, spatial patterns are largely absent in the proportions of F2, F1, C, B1 and B2 events. However, for mid-to-long durations, the proportion of very back-loaded events (B2) is notably higher in central and southern England and lower in Scotland, Wales, and along the southern and western coasts (Fig. 8). A similar, but less pronounced, pattern is observed for very front-loaded (F2) events (Fig. A.3). In contrast, the central categories (F1, C, B1) exhibit the opposite trend, with lower proportions in central and southern England and higher proportions across Scotland, Wales, and the southern and western coastal regions (Figs. A.4, A.5, A.6). The areas where events are more likely to be centred tend to correspond with those experiencing the latest event mean day-of-year. This pattern suggests that frontal rainfall, which tends to occur later in the year and to be more uniformly distributed, may play a more significant role in driving the annual maxima in these regions. In contrast, convective processes, which have previously been shown to be more dominant in central and southern areas by Darwish et al. (2018), may explain the higher occurrence of front-loaded events in those locations.

These spatial plots also allow us to begin to better characterise the changes to temporal loading happening in the future climate. We see that behind the overall 'no change' in temporal loading that individual locations are subject to changes in both directions. This is discussed further in Section 4.

3.6. Relationship between temporal loading and the event day-of-year

3.6.1. Overall findings

In the present climate, there is a discernible relationship between the day-of-year on which an event occurs, and its likelihood of having different temporal structures. Firstly, the top panel of Fig. 9a shows the proportion of all events occurring on each day of the year. There is a steady increase in the proportion of events occurring on a day, as we move from spring towards summer,

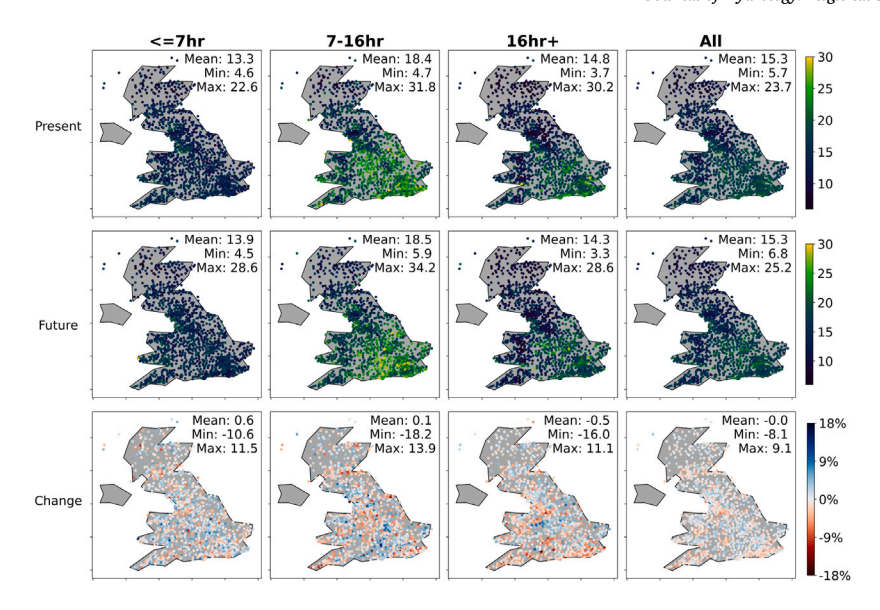


Fig. 8. The percentage of annual maxima extracted from UKCP Local climate simulations at grid box locations containing rain gauges classified as very back-loaded (B2). Results are displayed for present (2000–2019) and future climates (2060–2079), for all events and for three event duration categories.

and then a more gradual decrease towards winter. Secondly, the middle panel of Fig. 9a, presents a heat map visualisation of D_{50} values on each day of the year. This demonstrates that in the summer months events are fairly evenly distributed across the range of possible D_{50} values. Contrastingly, in winter and spring, there are higher proportions of more centred D_{50} values and temporal distributions. We note that the distinct, horizontal line in the middle of the heatmap plot reflects a tendency for events to cluster around a D_{50} value of 50. This is an artefact of the data resolution, which results in numerous events with a limited number of data points. Lastly, the bottom panel of Fig. 9a represents the proportion of events in each of the five quintile categories for each day of the year. Similarly, this shows that in late spring and summer events are fairly evenly distributed across the five categories, whilst in winter, early spring, and late autumn events tend to be in the more central quintile categories.

Fig. 9b presents similar plots to those in Fig. 9a but illustrates the differences between future and present climates. The top panel shows that in the future the proportion of events in summer and early autumn are smaller, whilst they are larger in winter and spring. The middle panel highlights changes in the proportion of events on each day corresponding to different D_{50} values, and the bottom panel shows changes for each quintile category. There are no consistent shifts observable in the likelihood of different temporal structures occurring at different times of year in the future. In the summer, we see little change in either direction, and during the rest of the year, both increases and decreases in the proportion of different D_{50} and quintile categories are observed. However, as discussed in Section 3.5.2, the mean D_{50} value and the proportion of events within the different quintile categories do exhibit shifts at certain locations. When data from all gauges are combined, these localised patterns become hidden, and identifying overall signals in the data is challenging.

3.6.2. Spatial patterns

Visual analysis reveals apparent similarities between the spatial patterns of the mean day-of-year of events (Fig. 5) and of the proportion of events classified as F2 (Fig. 8), in both present and future climates. To investigate this further, in Fig. 10 we assess the linear correlation between the mean day-of-year at each location and the proportion of events in the F2 category. We find a statistically significant (p < 0.05) negative relationship across all durations, indicating that locations where annual maxima occur later in the year tend to have a lower percentage of highly front-loaded (F2) events. This relationship is strongest for mid-duration events ($R^2 = 0.37$) and weakest for the longest-duration events ($R^2 = 0.17$).

We additionally explore the linear correlations between the mean event day-of-year and the other quintile categories (F1, C, B1, B2), as well as the mean D_{50} . For short durations, the correlations are statistically significant but weak. For mid- and long-duration events, the strength of the correlations are stronger, and support the idea that locations with annual maxima occurring later in the year tend to experience a higher percentage of more centred B1, C and F1 events, and a lower percentage of very back-loaded B2 events. For mean D_{50} , we observe a weak positive correlation with the mean event day-of-year.

In the future climate, the association between the mean event day-of-year and the proportion of events in different quintile categories becomes weaker. The negative relationship between later maxima and F2 events remains, but loses strength, with R^2 values ranging from 0.07 to 0.22. For mid- and long-duration events, the trends for centred (F1, C, B1) and highly asymmetrical (B2, F2) events are far less clear, suggesting a reduced influence of seasonality on event temporal loading. Interestingly, across all durations the correlation between mean event day-of-year and mean D_{50} increases in the future climate simulations.

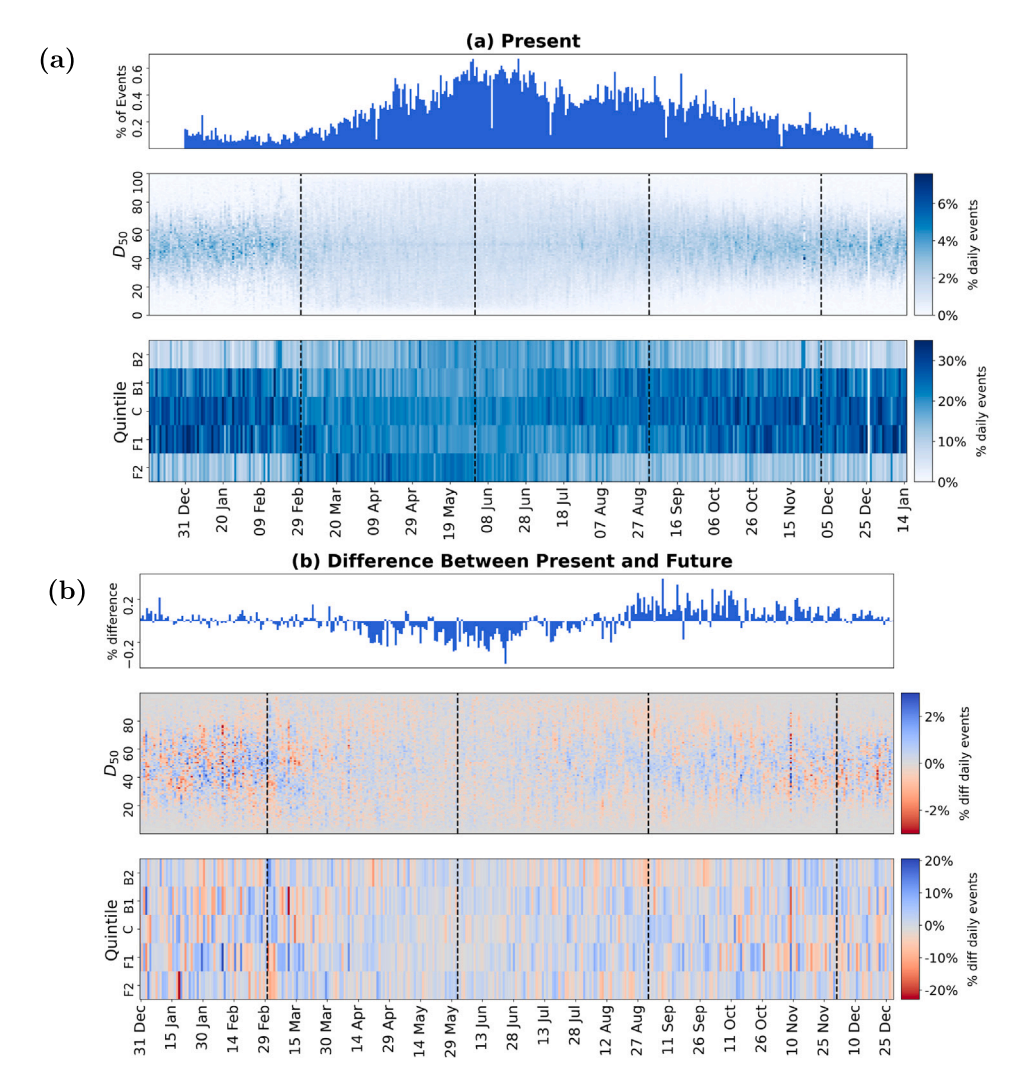


Fig. 9. Top panel: Bar plot of the proportion of the total number of annual events on each day of the year. Middle panel: Heat map showing the proportion of events on each day of the year classified as each of the D_{50} values from 1–100. Bottom panel: Heat map showing the proportion of events on each day of the year classified as each of the five quintile categories. (a) shows the proportion in the present day and (b) shows the proportion in the present minus the future.

Overall, the findings highlight a robust association between the timing of annual maxima and event symmetry, likely reflecting changes in the dominant event type throughout the year. For instance, more front-loaded convective events in summer, more backloaded frontal and orographic events in winter. However, the strength of the correlations suggest that seasonality alone explains only part of the variance in rainfall temporal distribution. Other geographical and meteorological factors likely contribute significantly to these patterns, highlighting the need for further investigation into additional drivers of event variability.

4. Summary and conclusions

This study investigates changes in the temporal loading of storms under future climates, enabled by the latest generation of convection-permitting climate models. These models offer improved representation of small-scale rainfall structures and event dynamics, allowing, for the first time, a detailed exploration of this previously unexamined aspect of rainfall variability in climate projections.

We extract annual maxima-producing rainstorms from the climate simulations and reproduce the well-established findings that extreme rainfall events become more intense and contain larger total event volumes under future climates. Additionally, we observe a clear trend towards annual maxima occurring later in the year and becoming more spread over the year. The analyses are performed at model grid cells where rain gauges are also located to allow comparison with the observational results of Villalobos Herrera et al. (2023a) for the same case area of Great Britain. Using the quintile classification method from Villalobos Herrera et al. (2023a),

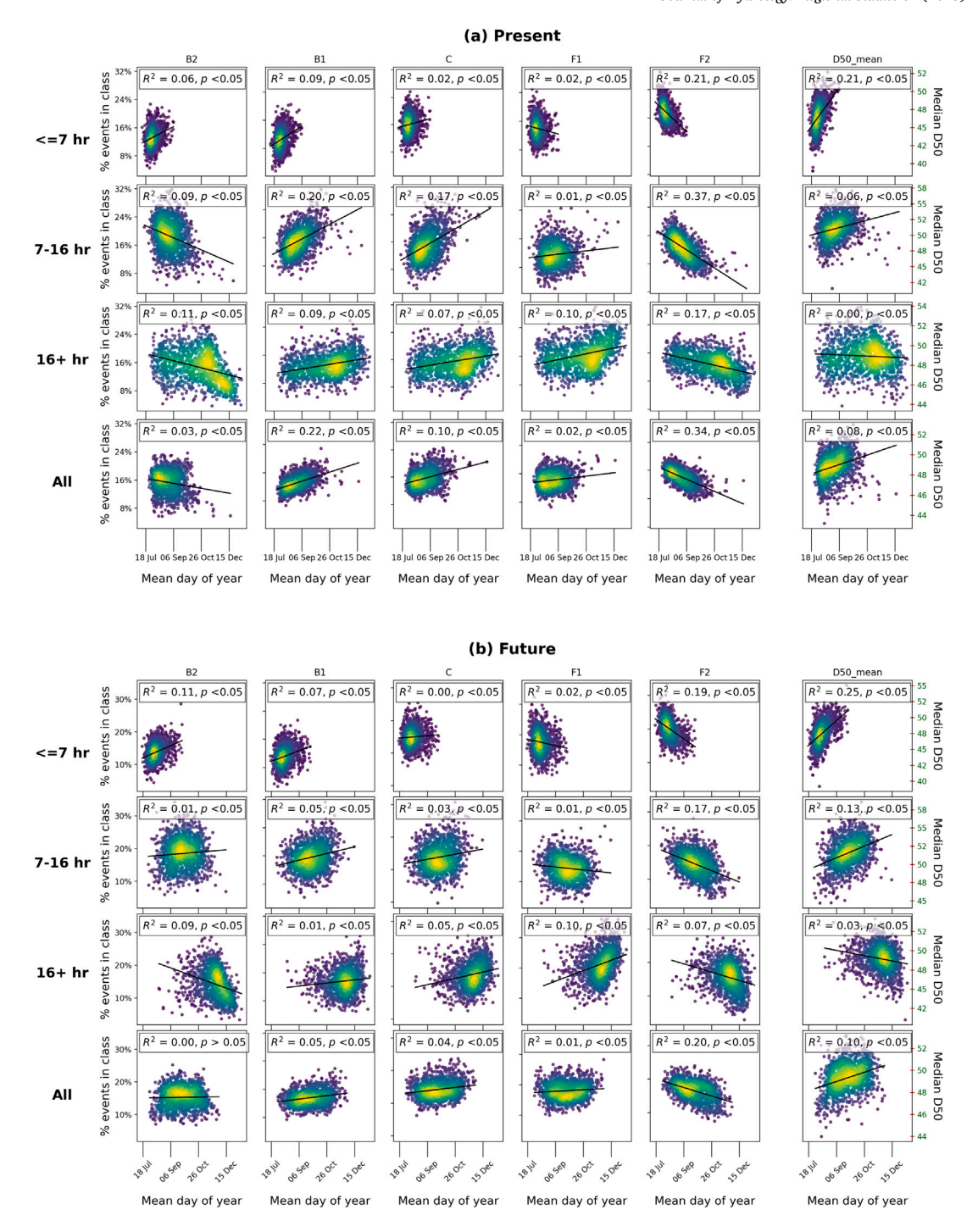


Fig. 10. Scatter plot of relationship between the mean day-of-year of annual maxima at each location, and temporal loading metrics. Each plot is annotated with the coefficient of determination, R^2 , and the p value, demonstrating the strength and statistical significance of the linear relationship. Results are displayed for present (2000–2019) and future climates (2060–2079), for all events and for three event duration categories.

we observe a tendency towards front-loading for shorter sampling durations, while at longer durations storms are more likely to have a more central peak in intensity in the climate model simulations. This aligns with the overarching conclusions drawn from study of annual maxima events from rain gauges (Villalobos Herrera et al., 2023a), providing crucial validation that UKCP Local realistically captures the temporal loading patterns observed in real-world rainfall events. Here, we also identify that these general trends mask considerable spatial variation in event loading. Across the longer durations especially, we observe lower proportions

of the most asymmetric loading categories around the western coastal areas and Scotland, and the highest proportions in central, southern England.

We do not identify substantial changes to the average temporal loading of annual maxima in future climates. This is in contrast to previous studies. For instance, Visser et al. (2023) applied the D_{50} metric to historical precipitation data, and through linking the results to temperature measurements, concluded that an increase in front-loading should be expected alongside climate warming. The same result was found for rain storms in the tropics by Ghanghas et al. (2024). One possible reason why our results do not support this conclusion is the focus of Visser et al. (2023) on Australian rainfall events. These events occur across diverse climate zones, including tropical regimes dominated by intense, short-duration convective storms, which are markedly different from the climate of Great Britain. They attribute the increased prevalence of front-loaded storms at higher temperatures to the inherent tendency of short-duration convective storms to be front-loaded, coupled with the greater frequency of such storms at higher temperatures, driven by heightened atmospheric instability and more vigorous cloud dynamics. Importantly, Ghanghas et al. (2024) find that in more temperate areas higher temperatures are conversely linked with more back-loading, attributing the regional difference to the influence of differing dominant storm mechanisms. Additionally, both Visser et al. (2023) and Ghanghas et al. (2024) study historical rainfall observations linked to temperature data, rather than future climate data. As established previously, evidence suggests that factors other than temperature influence event temporal loading, and this may be another reason for differences in our results.

If theory suggests that convective events may become more front-loaded, whilst frontal events become more back-loaded, detecting either signal will rely on the ability to distinguish between these storm types. In this research, we make a basic attempt to separate events by storm mechanism through grouping them into duration categories. Nevertheless, the observed spatial variability in temporal loading, as well as in the magnitude and direction of changes under future climates, suggests that even within these categories, different storm types may dominate in different regions. The existence of correlations between average event loading at a grid cell and the average time of year of occurrence, although weak, further supports this hypothesis. Our findings also indicate that annual maxima events occur later in the year in future climates, which we posit may result from either an extension of the convective season into autumn or an intensification of autumn and winter frontal events, leading to their increased dominance in the annual maxima collection. We recommend that future research explore more advanced methods for classifying storm types, such as those proposed by Dai et al. (2024) and Starzec et al. (2017), to enable more refined analysis and grouping.

Our ability to draw conclusions about changes in temporal loading under future climates is limited by the shortcomings of existing metrics. This research employs two methods: the quintile classification method (Villalobos Herrera et al., 2023a) and the D_{50} metric (Visser et al., 2023). Both, however, have significant limitations. The quintile method focuses solely on the highest rainfall portion of an event, disregarding the broader rainfall distribution. For instance, in a nearly uniform event where one value is slightly higher, the method classifies it as highly front-loaded, misrepresenting its symmetry. In contrast, the D_{50} metric incorporates the cumulative rainfall distribution, providing a more comprehensive measure of the event structure. However, it conflates event asymmetry with peak intensity, complicating its interpretation. For example, a more intense early peak moves D_{50} closer to 0, potentially suggesting a shift in peak timing rather than simply an increase in peak intensity. Conversely, if the peak occurs in the middle of an event, its magnitude has no influence on D_{50} , regardless of how pronounced it is. These nuances can obscure the underlying dynamics of storm events, and complicate interpretation of findings. For instance, Visser et al. (2023)'s finding of more front-loaded future storms in Australia could instead reflect the intensification of peaks shown in other studies to occur at higher temperatures (Wasko and Sharma, 2015). This highlights the need for more robust metrics which disentangle these effects and independently quantify asymmetry, peak timing, and intensity. Such metrics would enable clearer insights into how storms are expected to evolve under climate change, helping to resolve ambiguities and improve the reliability of climate impact assessments.

More robust metrics would not only enhance our understanding of how rainfall event temporal loading is likely to change in the future, but also help identify which components of these changes—such as asymmetry, peak intensity, or timing—matter most for flood risk. This is critical for informing and improving the design storm framework to ensure it incorporates those aspects of storm structure most relevant to flood impacts. For instance, existing research suggests that more severe flooding outcomes are associated with back-loaded storms, probably because earlier, lighter rainfall saturates and fills catchment's storage. However, this relationship may only hold for back-loaded storms with a very heavy rainfall burst at the end, a feature which is not a prerequisite to be classed as back-loaded in the quintile classification system applied in this research. Clarifying these distinctions would allow for the development of hyetograph profiles that are both scientifically robust and practically applicable, ensuring that design storms remain effective tools for managing flood risk in a changing climate.

CRediT authorship contribution statement

Molly Asher: Writing – review & editing, Writing – original draft, Visualization, Validation, Project administration, Methodology, Investigation, Formal analysis, Data curation, Conceptualization. Jonas Wied Pedersen: Writing – review & editing, Writing – original draft, Methodology, Conceptualization. Steven Böing: Validation, Supervision, Software, Data curation. Cathryn Birch: Writing – review & editing, Supervision, Funding acquisition. Mark Trigg: Writing – review & editing, Supervision, Project administration, Funding acquisition. Elizabeth Kendon: Resources.

Open research section

Data supporting this research are available in UKCP Local Convection-Permitting Model Projections for the UK at 2.2 km resolution (Met Office Hadley Centre, 2019), with restrictions due to licensing agreements. The 30-min resolution data used in this study are provided under licence from the Met Office and are not publicly accessible. An hourly version of the dataset is publicly available at https://catalogue.ceda.ac.uk/uuid/ad2ac0ddd3f34210b0d6e19bfc335539. Researchers seeking access to the 30-min data should contact the Met Office (enquiries@metoffice.gov.uk) to inquire about licensing terms and data access. Met Office Rain Radar Data from the NIMROD System are open source data published on the Centre for Environmental Data Analysis archive (Met Office, 2003), and available at: https://data.ceda.ac.uk/badc/ukmo-nimrod/data/composite/uk-1km.

Declaration of competing interest

The authors declare the following financial interests/personal relationships which may be considered as potential competing interests: Molly Asher reports was provided by University of Leeds. If there are other authors, they declare that they have no known competing financial interests or personal relationships that could have appeared to influence the work reported in this paper.

Acknowledgements

Molly Asher was funded by the Natural Environment Research Council, through the PANORAMA DTP [grant number: NE/S007458/1]

Jonas Wied Pedersen was financially supported by the Innovation Fund Denmark through the industrial postdoc program [grant number: 0197-00005B].

Cathryn Birch was funded by the Yorkshire Integrated Catchment Solutions Programme (iCASP, NERC grant number: NE/P011160/1).

Elizabeth Kendon was supported by the Met Office Hadley Centre Climate Programme funded by the Department for Science, Innovation and Technology.

We thank Dr. David Dufton at the University of Leeds for his insight and suggestions on working with NIMROD rain radar data.

Appendix A. Additional figures

See Figs. A.1-A.6.

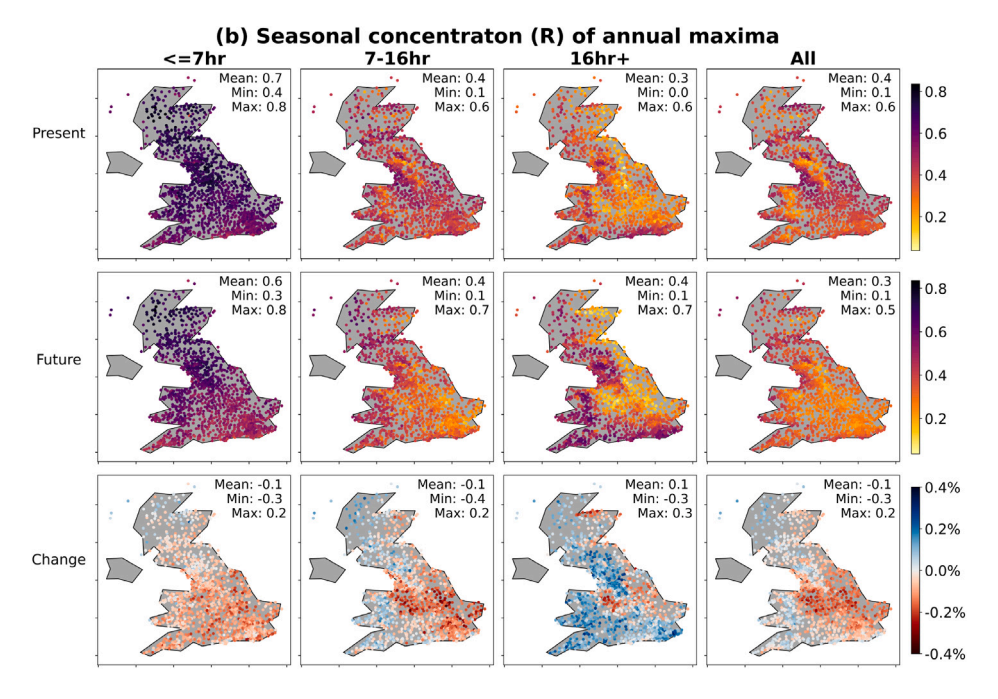


Fig. A.1. The R value (concentration of seasonal distribution) of annual maxima from UKCP18 climate simulations at grid box locations containing rain gauges. R values close to 1 show rainstorms very concentrated at a specific time of year. Results are displayed for present (2000–2019) and future climates (2060–2079), and the change between the two. Results are presented for all events and three event duration categories.

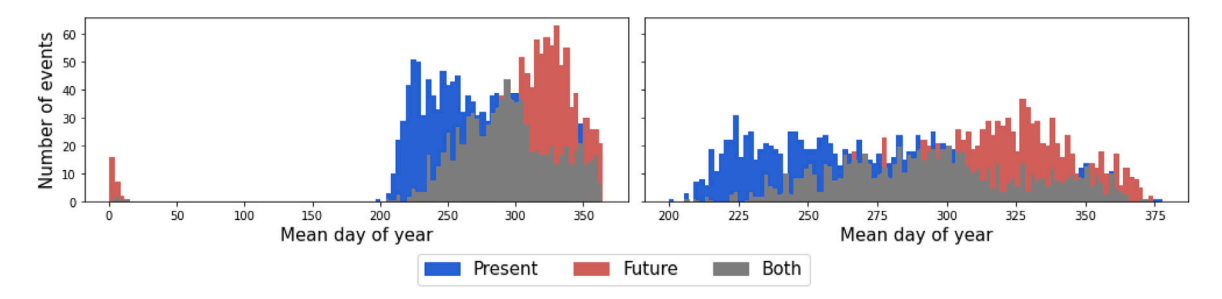


Fig. A.2. Histogram of (left) the mean day-of-the-year of events at locations, and (right) after adding 365 to January dates to make them appear at the end of the year, to more easily model linear relationships.

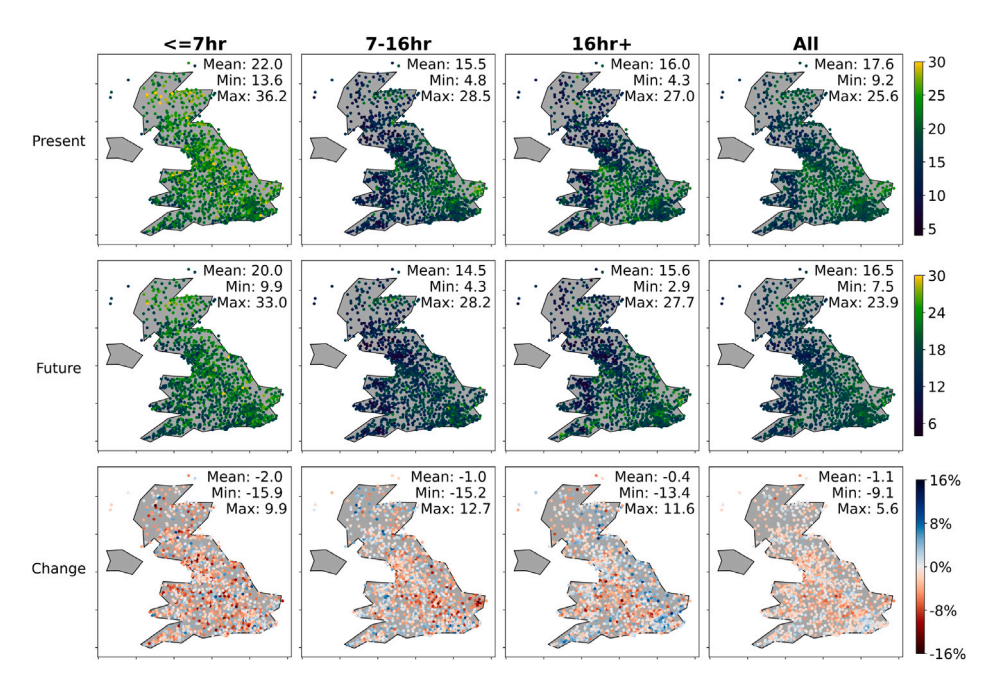


Fig. A.3. The percentage of annual maxima extracted from UKCP18 climate simulations at grid box locations containing rain gauges classified as very front-loaded (F2), for a present (2000–2019) and future climate (2060–2079). Results are presented for all events and three event duration categories.

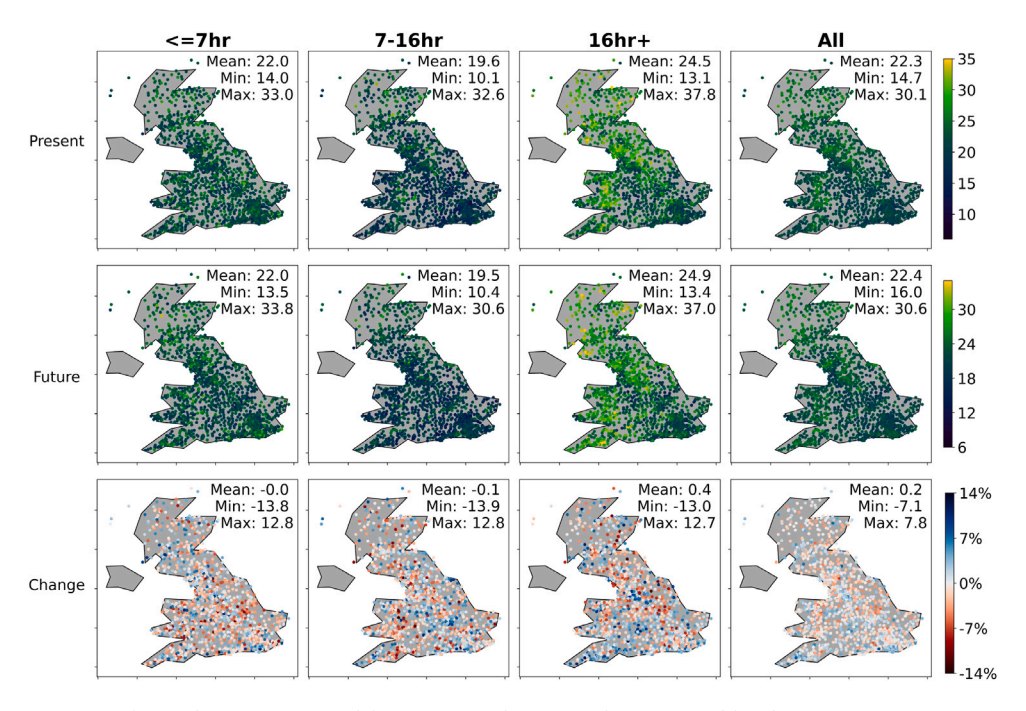


Fig. A.4. The percentage of annual maxima extracted from UKCP18 climate simulations at grid box locations containing rain gauges classified as front-loaded (F1), for a present (2000–2019) and future climate (2060–2079). Results are presented for all events and three event duration categories.

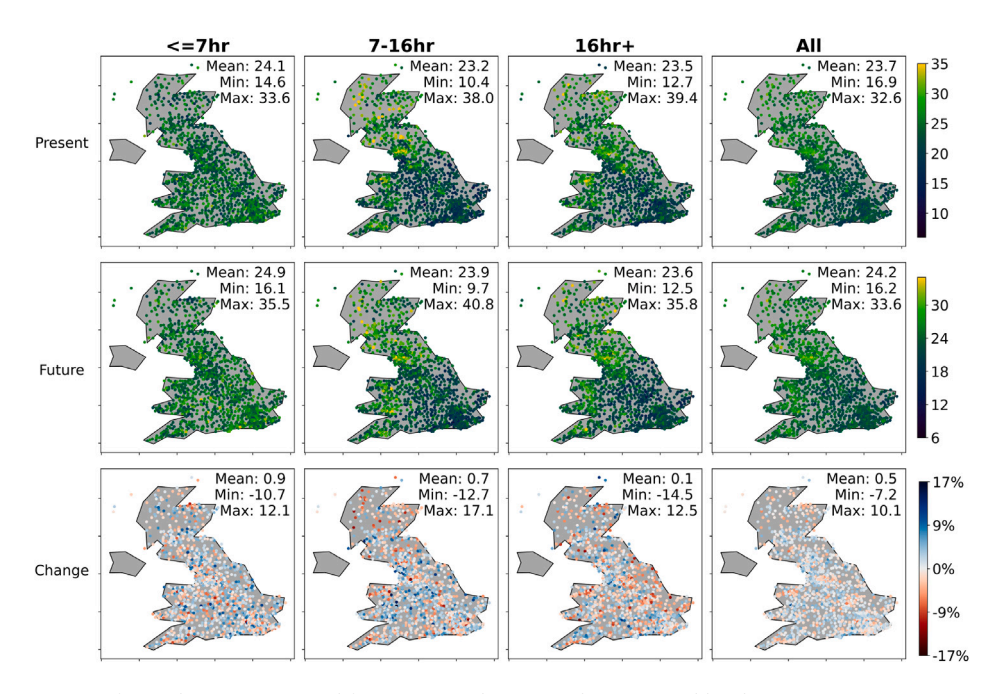


Fig. A.5. The percentage of annual maxima extracted from UKCP18 climate simulations at grid box locations containing rain gauges classified as centred (C), for a present (2000–2019) and future climate (2060–2079). Results are presented for all events and three event duration categories.

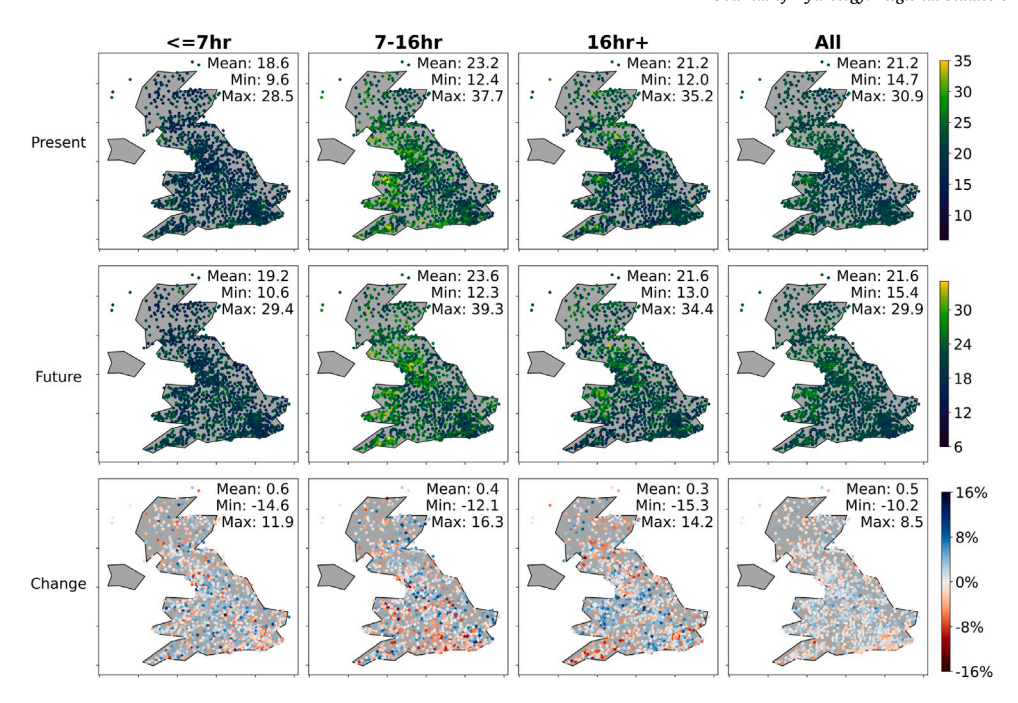


Fig. A.6. The percentage of annual maxima extracted from UKCP18 climate simulations at grid box locations containing rain gauges classified as back-loaded (B1), for a present (2000–2019) and future climate (2060–2079). Results are presented for all events and three event duration categories.

Appendix B. Supplementary data

Supplementary material related to this article can be found online at https://doi.org/10.1016/j.ejrh.2025.102750.

Data availability

The authors do not have permission to share data.

References

Archer, L., Hatchard, S., Devitt, L., Neal, J., Coxon, G., Bates, P., Kendon, E., Savage, J., 2024. Future change in urban flooding using new convection-permitting climate projections. Water Resour. Res. 60 (1), e2023WR035533.

Asher, M., Trigg, M., Boïng, S., Birch, C., 2025. The sensitivity of urban pluvial flooding to the temporal distribution of rainfall within design storms. J. Flood Risk Manage. 18 (3), e70097.

Balbastre-Soldevila, R., García-Bartual, R., Andrés-Doménech, I., 2019. A comparison of design storms for urban drainage system applications. Water 11 (4), 757. Ball, J., Babister, M., Nathan, R., Weinmann, P., Weeks, W., Retallick, M., Testoni, I., 2019. Australian rainfall and runoff-a guide to flood estimation.

Ban, N., Schmidli, J., Schär, C., 2014. Evaluation of the convection-resolving regional climate modeling approach in decade-long simulations. J. Geophys. Res.: Atmospheres 119 (13), 7889–7907.

Barbero, R., Fowler, H., Lenderink, G., Blenkinsop, S., 2017. Is the intensification of precipitation extremes with global warming better detected at hourly than daily resolutions? Geophys. Res. Lett. 44 (2), 974–983.

Bayliss, A., Jones, R., 1993. Peaks-Over-Threshold Flood Database: Summary Statistics and Seasonality. Technical Report, Institute of Hydrology, Wallingford, UK.

Berthou, S., Roberts, M.J., Vannière, B., Ban, N., Belušić, D., Caillaud, C., Crocker, T., de Vries, H., Dobler, A., Harris, D., et al., 2022. Convection in future winter storms over Northern Europe. Environ. Res. Lett. 17 (11), 114055.

Blenkinsop, S., Fowler, H.J., 2014. An hourly and multi-hourly extreme precipitation climatology for the UK and long-term changes in extremes. In: 2nd International Conference on Vulnerability and Risk Analysis and Management (ICVRAM) and the 6th International Symposium on Uncertainty Modeling and Analysis. ISUMA, Liverpool, UK, http://dx.doi.org/10.1061/9780784413609.139.

Blenkinsop, S., Lewis, E., Chan, S.C., Fowler, H.J., 2016. Quality-control of an hourly rainfall dataset and climatology of extremes for the UK. Int. J. Climatol. 37 (2), 722.

Bonta, J., Shahalam, A., 2003. Cumulative storm rainfall distributions: comparison of Huff curves. J. Hydrol. (New Zealand) 65-74.

Chan, S.C., Kendon, E.J., Berthou, S., Fosser, G., Lewis, E., Fowler, H.J., 2020. Europe-wide precipitation projections at convection permitting scale with the unified model. Clim. Dyn. 55, 409–428.

Chan, S.C., Kendon, E.J., Fowler, H.J., Youngman, B.D., Dale, M., Short, C., 2023. New extreme rainfall projections for improved climate resilience of urban drainage systems. Clim. Serv. 30, 100375.

- Chan, S., Kendon, E., Roberts, N., Fowler, H., Blenkinsop, S., 2016. The characteristics of summer sub-hourly rainfall over the southern UK in a high-resolution convective permitting model. Environ. Res. Lett. 11 (9), 094024.
- Chen, Y., Paschalis, A., Kendon, E., Kim, D., Onof, C., 2021. Changing spatial structure of summer heavy rainfall, using convection-permitting ensemble. Geophys. Res. Lett. 48 (3), e2020GL090903.
- Cotterill, D.F., Pope, J.O., Stott, P.A., 2023. Future extension of the UK summer and its impact on autumn precipitation. Clim. Dyn. 60 (5), 1801-1814.
- Cotterill, D., Stott, P., Christidis, N., Kendon, E., 2021. Increase in the frequency of extreme daily precipitation in the United Kingdom in autumn. Weather. Clim. Extrem. 33, 100340.
- Dai, G., Yang, B., Huang, D., Yang, Z., Tang, J., Qian, Y., Zhang, Y., 2024. On the relationship between precipitation extreme and local temperature over eastern China based on convection permitting simulations: roles of different moisture processes and precipitation types. Clim. Dyn. 1–16.
- Dales, M., Reed, D., 1989. Regional Flood and Storm Hazard Assessment. Institute of Hydrology.
- Darwish, M.M., Fowler, H.J., Blenkinsop, S., Tye, M.R., 2018. A regional frequency analysis of UK sub-daily extreme precipitation and assessment of their seasonality. Int. J. Climatol. 38 (13), 4758–4776.
- Dunkerley, D., 2008. Identifying individual rain events from pluviograph records: a review with analysis of data from an Australian dryland site. Hydrol. Process.: An Int. J. 22 (26), 5024–5036.
- Dunkerley, D., 2021. The importance of incorporating rain intensity profiles in rainfall simulation studies of infiltration, runoff production, soil erosion, and related landsurface processes. J. Hydrol. 603, 126834.
- Eagleson, P.S., 1970. Dynamic Hydrology. McGraw-Hill, New York.
- Fadhel, S., Rico-Ramirez, M.A., Han, D., 2018. Sensitivity of peak flow to the change of rainfall temporal pattern due to warmer climate. J. Hydrol. 560, 546–559. Fan, L., Lehmann, P., Zheng, C., Or, D., 2020. Rainfall intensity temporal patterns affect shallow landslide triggering and hazard evolution. Geophys. Res. Lett. 47 (1), e2019GL085994.
- Fosser, G., Kendon, E.J., Stephenson, D., Tucker, S., 2020. Convection-permitting models offer promise of more certain extreme rainfall projections. Geophys. Res. Lett. e2020GL088151.
- Fosser, G., Khodayar, S., Berg, P., 2015. Benefit of convection permitting climate model simulations in the representation of convective precipitation. Clim. Dyn. 44, 45–60.
- Fowler, H.J., Lenderink, G., Prein, A.F., Westra, S., Allan, R.P., Ban, N., Barbero, R., Berg, P., Blenkinsop, S., Do, H.X., et al., 2021. Anthropogenic intensification of short-duration rainfall extremes. Nat. Rev. Earth Environ. 2 (2), 107–122.
- Fu, X., Liu, J., Mei, C., Luan, Q., Wang, H., Shao, W., Sun, P., Huo, Y., 2021. Effect of typhoon rainstorm patterns on the spatio-temporal distribution of non-point source pollution in a coastal urbanized watershed. J. Clean. Prod. 292, 126098.
- Gao, G., Liang, Y., Liu, J., Dunkerley, D., Fu, B., 2024. A modified RUSLE model to simulate soil erosion under different ecological restoration types in the loess hilly area. Int. Soil Water Conserv. Res. 12 (2), 258–266.
- García-Bartual, R., Andrés-Doménech, I., 2017. A two-parameter design storm for mediterranean convective rainfall. Hydrol. Earth Syst. Sci. 21 (5), 2377–2387. Ghanghas, A., Sharma, A., Merwade, V., 2024. Unveiling the evolution of extreme rainfall storm structure across space and time in a warming climate. Earth's Futur. 12 (9), e2024EF004675.
- Gillett, N., Fyfe, J., 2013. Annular mode changes in the CMIP5 simulations. Geophys. Res. Lett. 40 (6), 1189-1193.
- Grabowski, W.W., Prein, A.F., 2019. Separating dynamic and thermodynamic impacts of climate change on daytime convective development over land. J. Clim. 32 (16), 5213–5234.
- Haerter, J., Berg, P., Hagemann, S., 2010. Heavy rain intensity distributions on varying time scales and at different temperatures. J. Geophys. Res.: Atmospheres 115 (D17).
- Hall, J., Blöschl, G., 2018. Spatial patterns and characteristics of flood seasonality in Europe. Hydrol. Earth Syst. Sci. 22 (7), 3883-3901.
- Harrison, D., Driscoll, S., Kitchen, M., 2000. Improving precipitation estimates from weather radar using quality control and correction techniques. Meteorol. Appl. 7 (2), 135–144.
- Harrison, D.L., Norman, K., Pierce, C., Gaussiat, N., 2012. Radar products for hydrological applications in the UK. In: Proceedings of the Institution of Civil Engineers-Water Management. vol. 165, Thomas Telford Ltd, pp. 89–103.
- Hathaway, J., Bean, E., Bernagros, J., Christian, D., Davani, H., Ebrahimian, A., Fairbaugh, C., Gulliver, J., McPhillips, L., Palino, G., et al., 2024. A synthesis of climate change impacts on stormwater management systems: Designing for resiliency and future challenges. J. Sustain. Water Built Environ. 10 (2), 04023014.
- Hettiarachchi, S., Wasko, C., Sharma, A., 2018. Increase in flood risk resulting from climate change in a developed urban watershed-the role of storm temporal patterns. Hydrol. Earth Syst. Sci. 22 (3), 2041–2056.
- Huff, F.A., 1967. Time distribution of rainfall in heavy storms. Water Resour. Res. 3 (4), 1007-1019.
- Jones, M.R., Fowler, H.J., Kilsby, C.G., Blenkinsop, S., 2013. An assessment of changes in seasonal and annual extreme rainfall in the UK between 1961 and 2009. Int. J. Climatol. 33 (5), 1178–1194.
- Jun, C., Qin, X., Chen, M., Seo, H., 2021. Investigating event-based temporal patterns of design rainfall in a tropical region. Hydrol. Sci. J. 66 (13), 1986–1996. Kendon, E.J., Ban, N., Roberts, N.M., Fowler, H.J., Roberts, M.J., Chan, S.C., Evans, J.P., Fosser, G., Wilkinson, J.M., 2017. Do convection-permitting regional climate models improve projections of future precipitation change? Bull. Am. Meteorol. Soc. 98 (1), 79–93.
- Kendon, E.J., Fischer, E.M., Short, C.J., 2023. Variability conceals emerging trend in 100yr projections of UK local hourly rainfall extremes. Nat. Commun. 14
- Kendon, E., Fosser, G., Murphy, J., Chan, S., Clark, R., Harris, G., Lock, A., Lowe, J., Martin, G., Pirret, J., Roberts, N., Sanderson, M., Tucker, S., 2019. UKCP Convection-Permitting Model Projections: Science Report. Technical Report, UK Met Office, Exeter, UK, p. 153, URL https://www.metoffice.gov.uk/pub/data/weather/uk/ukcp18/science-reports/UKCP-Convection-permitting-model-projections-report.pdf.
- Kendon, E.J., Roberts, N.M., Fowler, H.J., Roberts, M.J., Chan, S.C., Senior, C.A., 2014. Heavier summer downpours with climate change revealed by weather forecast resolution model. Nat. Clim. Chang. 4 (7), 570–576.
- Kottegoda, N., Kassim, A., 1991. Classification of storm profiles using crossing properties. J. Hydrol. 127 (1-4), 37-53.
- Krvavica, N., Rubinić, J., 2020. Evaluation of design storms and critical rainfall durations for flood prediction in partially urbanized catchments. Water 12 (7), 2044.
- Lambourne, J., Stephenson, D., 1987. Model study of the effect of temporal storm distributions on peak discharges and volumes. Hydrol. Sci. J. 32 (2), 215–226. Ledingham, J., Archer, D., Lewis, E., Fowler, H., Kilsby, C., 2019. Contrasting seasonality of storm rainfall and flood runoff in the UK and some implications for rainfall-runoff methods of flood estimation. Hydrol. Res. 50 (5), 1309–1323.
- Lee, J.-Y., Marotzke, J., Bala, G., Cao, L., Corti, S., Dunne, J.P., Engelbrecht, F., Fischer, E., Fyfe, J.C., Jones, C., et al., 2021. Future global climate: scenario-based projections and near-term information. In: Climate Change 2021: The Physical Science Basis. Contribution of Working Group I To the Sixth Assessment Report of the Intergovernmental Panel on Climate Change. Cambridge University Press, pp. 553–672.
- Lenderink, G., Van Meijgaard, E., 2009. Unexpected rise in extreme precipitation caused by a shift in rain type? Nat. Geosci. 2 (6), 373-373.
- Lewis, E., Quinn, N., Blenkinsop, S., Fowler, H.J., Freer, J., Tanguy, M., Hitt, O., Coxon, G., Bates, P., Woods, R., 2018. A rule based quality control method for hourly rainfall data and a 1 km resolution gridded hourly rainfall dataset for great britain: CEH-GEAR1hr. J. Hydrol. 564, 930–943.
- Li, T., Lee, G., Kim, G., 2021. Case study of urban flood inundation—Impact of temporal variability in rainfall events. Water 13 (23), 3438.

Liu, J., Liang, Y., Gao, G., Dunkerley, D., Fu, B., 2022. Quantifying the effects of rainfall intensity fluctuation on runoff and soil loss: From indicators to models. J. Hydrol. 607, 127494.

Long, K., Wang, D., Wang, G., Zhu, J., Wang, S., Xie, S., 2021. Higher temperature enhances spatiotemporal concentration of rainfall. J. Hydrometeorol. 22 (12), 3159–3169

Mardia, K.V., 1975. Statistics of directional data. J. R. Stat. Soc. Ser. B Stat. Methodol. 37 (3), 349-371.

McKenna, C.M., Maycock, A., 2022. The role of the North Atlantic Oscillation for projections of winter mean precipitation in Europe. Geophys. Res. Lett. 49 (19), e2022GL099083.

Met Office, 2003. Met office rain radar data from the NIMROD system. URL http://catalogue.ceda.ac.uk/uuid/82adec1f896af6169112d09cc1174499/. (Accessed October 2024).

Met Office Hadley Centre, 2019. UKCP18 convection-permitting model projections for the UK at 2.2 km resolution. NERC EDS Cent. Environ. Data Anal..

Molina-Sanchis, I., Lázaro, R., Arnau-Rosalén, E., Calvo-Cases, A., 2016. Rainfall timing and runoff: The influence of the criterion for rain event separation. J. Hydrol. Hydromech. 64 (3), 226–236.

Müller, T., Schütze, M., Bárdossy, A., 2017. Temporal asymmetry in precipitation time series and its influence on flow simulations in combined sewer systems. Adv. Water Resour. 107, 56–64.

Murphy, J., Harris, G., Sexton, D., Kendon, E., Bett, P., Clark, R., Eagle, K., Fosser, G., Fung, F., Lowe, J., McDonald, R., McInnes, R., McSweeney, C., Mitchell, J., Rostron, J., Thornton, H., Tucker, S., Yamazaki, K., 2018. UKCP18 Land Projections: Science Report. Technical Report, UK Met Office, Exeter, UK.

Nguyen, V.-T.-V., Peyron, N., Rivard, G., 2002. Rainfall temporal patterns for urban drainage design in southern quebec. In: Proceedings of the Ninth International Conference on Urban Drainage. Portland, Oregon, p. 16.

Peleg, N., Skinner, C., Fatichi, S., Molnar, P., 2020. Temperature effects on the spatial structure of heavy rainfall modify catchment hydro-morphological response. Earth Surf. Dyn. 8 (1), 17–36.

Pendergrass, A.G., 2018. What precipitation is extreme? Science 360 (6393), 1072-1073.

Pilgrim, D., Cordery, I., French, R., 1969. Temporal patterns of design rainfall for sydney. Civ. Eng. Trans. 9-14.

Prein, A.F., Langhans, W., Fosser, G., Ferrone, A., Ban, N., Goergen, K., Keller, M., Tölle, M., Gutjahr, O., Feser, F., et al., 2015. A review on regional convection-permitting climate modeling: Demonstrations, prospects, and challenges. Rev. Geophys. 53 (2), 323–361.

Prosdocimi, I., Kjeldsen, T., Svensson, C., 2014. Non-stationarity in annual and seasonal series of peak flow and precipitation in the UK. Nat. Hazards Earth Syst. Sci. 14 (5), 1125–1144.

Rahman, A., Weinmann, P.E., Hoang, T.M.T., Laurenson, E.M., 2002. Monte Carlo simulation of flood frequency curves from rainfall. J. Hydrol. 256 (3-4), 196-210

Reed, D., Robson, A., 1999. Flood Estimation Handbook, vol. 3, Institute of Hydrology Wallingford.

Restrepo-Posada, P.J., Eagleson, P.S., 1982. Identification of independent rainstorms. J. Hydrol. 55 (1-4), 303-319.

Schär, C., Ban, N., Fischer, E.M., Rajczak, J., Schmidli, J., Frei, C., Giorgi, F., Karl, T.R., Kendon, E.J., Tank, A.M.K., et al., 2016. Percentile indices for assessing changes in heavy precipitation events. Clim. Change 137, 201–216.

Sexton, D.M., McSweeney, C.F., Bett, P.E., Fung, F., Thornton, H.E., Yamazaki, K., 2024. Describing future UK winter precipitation in terms of changes in local circulation patterns. Clim. Dyn. 1–19.

Sharma, A., Hettiarachchi, S., Wasko, C., 2021. Estimating design hydrologic extremes in a warming climate: alternatives, uncertainties and the way forward. Phil. Trans. R. Soc. A 379 (2195), 20190623.

Starzec, M., Homeyer, C.R., Mullendore, G.L., 2017. Storm labeling in three dimensions (SL3D): A volumetric radar echo and dual-polarization updraft classification algorithm. Mon. Weather Rev. 145 (3), 1127–1145.

Stephenson, D., Pavan, V., Collins, M., Junge, M., Quadrelli, R., Groups, P.C.M., 2006. North atlantic oscillation response to transient greenhouse gas forcing and the impact on European winter climate: a CMIP2 multi-model assessment. Clim. Dyn. 27, 401–420.

Todisco, F., 2014. The internal structure of erosive and non-erosive storm events for interpretation of erosive processes and rainfall simulation. J. Hydrol. 519, 3651–3663

Trenberth, K.E., Dai, A., Rasmussen, R.M., Parsons, D.B., 2003. The changing character of precipitation. Bull. Am. Meteorol. Soc. 84 (9), 1205–1218.

UK Met Office, 2024. UKCP Guidance: Extreme Rainfall Features in UKCP Local. Technical Report, UK Met Office, Exeter, UK, URL https://www.metoffice.gov.uk/binaries/content/assets/metofficegovuk/pdf/research/ukcp/ukcp18_guidance_extreme_rainfall.pdf. Met Office 00A9 Crown Copyright 2024.

Villalobos Herrera, R., Blenkinsop, S., Guerreiro, S.B., Dale, M., Faulkner, D., Fowler, H.J., 2023a. Towards new design rainfall profiles for the United Kingdom. J. Flood Risk Manag. e12958.

Villalobos Herrera, R., Blenkinsop, S., Guerreiro, S.B., Fowler, H.J., 2023b. The creation and climatology of a large independent rainfall event database for Great Britain. Int. J. Climatol. 43 (13), 6020–6037.

Villarini, G., 2016. On the seasonality of flooding across the continental United States. Adv. Water Resour. 87, 80-91.

Visser, J.B., Wasko, C., Sharma, A., Nathan, R., 2023. Changing storm temporal patterns with increasing temperatures across Australia. J. Clim. 36 (18), 6247–6259.

Vrac, M., Vaittinada Ayar, P., Yiou, P., 2014. Trends and variability of seasonal weather regimes. Int. J. Climatol. 34 (2).

Walters, D., Baran, A.J., Boutle, I., Brooks, M., Earnshaw, P., Edwards, J., Furtado, K., Hill, P., Lock, A., Manners, J., et al., 2019. The met office unified model global atmosphere 7.0/7.1 and JULES global land 7.0 configurations. Geosci. Model. Dev. 12 (5), 1909–1963.

Wang, F., 2020. Temporal pattern analysis of local rainstorm events in China during the flood season based on time series clustering. Water 12 (3), 725.

Wang, H., Chen, R., Leung, A.K., Garg, A., 2023. Hydrological responses to early-peak rainfall in unsaturated rooted soils. Heliyon 9 (5).

Wang, W., Yin, S., Xie, Y., Liu, B., Liu, Y., 2016. Effects of four storm patterns on soil loss from five soils under natural rainfall. Catena 141, 56-65.

Wasko, C., Sharma, A., 2015. Steeper temporal distribution of rain intensity at higher temperatures within Australian storms. Nat. Geosci. 8 (7), 527-529.

Watt, E., Marsalek, J., 2013. Critical review of the evolution of the design storm event concept. Can. J. Civ. Eng. 40 (2), 105–113.

Westra, S., Fowler, H.J., Evans, J.P., Alexander, L.V., Berg, P., Johnson, F., Kendon, E.J., Lenderink, G., Roberts, N., 2014. Future changes to the intensity and frequency of short-duration extreme rainfall. Rev. Geophys. 52 (3), 522–555.

Zhao, B., Marin, R.J., Luo, W., Yu, Z., Yuan, L., 2025. Rainfall thresholds for shallow landslides considering rainfall temporal patterns. Bull. Eng. Geol. Environ. 84 (3), 1–13.